

Doctoral thesis

Doctoral theses at NTNU, 2021:224

Jan Sramota

Industry 4.0

Monitoring the Condition of Railway
Turnouts

NTNU
Norwegian University of Science and Technology
Thesis for the Degree of
Philosophiae Doctor
Faculty of Engineering
Department of Mechanical and Industrial
Engineering



Norwegian University of
Science and Technology

Jan Sramota

Industry 4.0

Monitoring the Condition of Railway Turnouts

Thesis for the Degree of Philosophiae Doctor

Trondheim, June 2021

Norwegian University of Science and Technology
Faculty of Engineering
Department of Mechanical and Industrial Engineering



Norwegian University of
Science and Technology

NTNU

Norwegian University of Science and Technology

Thesis for the Degree of Philosophiae Doctor

Faculty of Engineering

Department of Mechanical and Industrial Engineering

© Jan Sramota

ISBN 978-82-326-6121-3 (printed ver.)

ISBN 978-82-326-6488-7 (electronic ver.)

ISSN 1503-8181 (printed ver.)

ISSN 2703-8084 (online ver.)

Doctoral theses at NTNU, 2021:224

Printed by NTNU Grafisk senter

To Mother Nature in hope for better tomorrows...

Summary

Ensuring safety is by far the most important reason for maintaining railway systems. Faults and defects detected early on can in addition be remedied before they cause a service stoppage which is a partial reason why the railway industry is starting to use new digital systems for monitoring important track assets. While many track components can be inspected effectively by the methods used to date, those for the surveillance of particular elements such as railway turnouts are less effective, and new systems have yet to be developed. Due to the large number of turnouts in the railway infrastructure, which is estimated to average one per kilometre of track, these systems must be economically viable and satisfy all the parameters required, which can be particularly demanding.

This thesis presents a system intended for the remote monitoring of railway turnouts, developed during this doctoral study. The system consists of track-side wireless sensors, a gateway and a server. The wireless sensors are attached to the rails and comprise a digital accelerometer, a battery and a communication module, and sense vibration as trains pass over them. When required, the wireless sensors record the vehicle-track interaction and send it wirelessly to the nearby gateway, which forwards the data collected to the server where they are aggregated, analysed and stored. When a defect on the track is identified, relevant trains receive this information immediately via a direct communication channel or indirectly through other infrastructure as programmable balises. Strong integration with existing communication networks and the surrounding infrastructure result in low overall costs for the deployment, operation and maintenance of this system.

The system's usability and performance were assessed on tracks in Denmark and Germany. This revealed issues that made it unsuitable for efficient use on a large scale. Following revision, deficiencies were removed and the system named RailCheck was deployed on the most occupied section of Norway's railway network. Data from a double crossover turnout were collected and released for non-commercial academic and research use as the RailCheck dataset. These data are now available and can be studied for a better understanding of transient events between vehicle-track interactions present in non-ideal datasets, and can be used as a basis for simulations, algorithm development and method verification. This may eventually lead to the creation of reliable algorithms that can be directly applied to real-time measurement systems, enabling autonomous analysis of the state of the track as required for a successful transition to predictive maintenance.

This thesis comprises six chapters, each of which describes a formal milestone that was required in order to continue the work presented in the next chapter. Since the project was redesigned several times as local railway administrations requirements changed and we gained experience and knowledge, the project followed the standard life cycle of system development: definition, analysis, realisation, and evaluation, as shown in Fig. 1 and described in the following chapters:

- Chapter 1, Introduction—describes the formal requirements for this doctoral study, and defines the project and the reasons for our decision to work on this project.
- Chapter 2, Background—summarises the most common railway track defects and describes how they can be effectively detected and resolved.
- Chapter 3, Analysis—introduces the proposed solution for monitoring turnouts using the wireless sensor network (WSN) and low-power wide-area network (LPWAN) concept, with the foundational ideas and calculations.
- Chapter 4, Realisation—discusses the design and manufacturing processes, describing the development of the hardware and the software for each component in detail.
- Chapter 5, Evaluation—outlines some of the problems that arose during the development of the RailCheck system and its testing, and how we dealt with them.
- Chapter 6, Conclusion—summarises the results obtained during the three years of the doctoral study, not including the assignments required to acquire 34 European Credit Transfer and Accumulation System (ECTS) credits.

The thesis also includes schematics, published articles and other additions that resulted from this project and are attached in [Appendices](#).

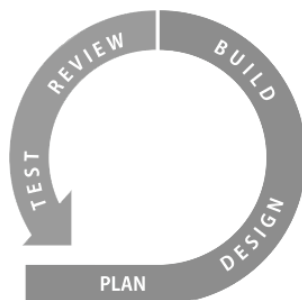


Figure 1: System development life cycle

Contents

Summary	ii
Contents	iv
List of figures	viii
List of tables	x
List of abbreviations	xii
1 Introduction	1
1.1 DESTination RAIL Project	2
1.2 Research Objectives	3
1.3 Scope	3
1.4 Motivation	4
1.5 Contributions	4
1.6 Publications	4
2 Background	6
2.1 Rail Defects	6
2.1.1 Rolling Contact Fatigue Defects	6
2.1.2 Other Defects	6
2.2 Rail Maintenance	8
2.2.1 Rail Grinding	8
2.2.2 Rail Tamping	9
2.2.3 Rail Replacement	9
3 Analysis	10
3.1 Wireless Sensor	11
3.1.1 Sensors	11
3.1.2 Communication	14

3.1.3	Memory and Processing	15
3.1.4	Power Management	16
3.1.5	Mechanical Casing	19
3.2	Gateway (& Cloud)	20
3.3	Server	20
4	Realisation	22
4.1	Wireless Sensor	23
4.2	Gateway	25
4.3	Server	26
5	Evaluation	28
5.1	Preliminary and Laboratory Measurements	28
5.1.1	Concept Feasibility Test	28
5.1.2	Bottleneck on IQRF Cloud	30
5.2	Measurements in Denmark	31
5.2.1	Communication Gateway–CMS (Issue #1)	31
5.2.2	Communication Wireless Sensors–Gateway (Issue #2)	31
5.3	Measurements in Germany	31
5.3.1	Rail Coverage Test	32
5.4	Measurements in Norway	33
5.4.1	ADXL372 External Clock Prescaler (Issue #1)	33
5.4.2	ADXL372 FFT ODR/5 Noise (Issue #2)	34
5.4.3	ADXL372 Data Misalignment in FIFO Stream Mode (Bug #1)	34
6	Conclusion	36
	References	38
	Appendices	41
	<hr/>	
A	Publications	43
A.1	RailCheck: A WSN-Based System for Condition Monitoring of Railway Infrastructure	44
A.2	RailCheck: Functional Safety for Wireless Condition Monitoring of Railway Turnouts and Level Crossings	50
A.3	RailCheck Dataset of Vehicle-Track Interaction Measured on Railway Turnouts	58
B	Schematic	67
B.1	Wireless Sensor Hardware v1.0	68

B.2	Wireless Sensor Hardware v1.1	70
B.3	Norwegian Railway Network	72
B.4	Various Amendments	74
C	Photos	77
C.1	Wireless Sensor (PCB, WSC)	78
C.2	Content Management System (CMS)	82
C.3	Antenna Test	86
C.4	Coverage Test	88
C.5	Measurement Denmark	92
C.6	Measurement Germany	96
C.7	Measurement Oslo	100

List of figures

- 1 System development life cycle iii
- 2.1 Rail defects 7
- 2.2 Rail maintenance 8
- 3.1 Proposed concept 10
- 3.2 IQRF TR-76D 15
- 3.3 Installation of wireless sensor on a rail 19
- 3.4 IQRF topology 20
- 4.1 Wireless sensor PCB v1.0 and v1.1 23
- 4.2 Wireless sensor casing v1.1 24
- 4.3 Wireless sensor—compression code v1.0.3 (simplified) 25
- 4.4 Gateway v1.0 and v1.1 26
- 5.1 Feasibility test on a rails in Trondheim 29
- 5.2 IQRF Cloud bottleneck 30
- 5.3 ADXL372 schema 34
- 5.4 ADXL372 data misalignment bug 35
- B.1 Various amendments 75
- C.1 Wireless sensor v1.0 79
- C.2 Wireless sensor v1.1 81
- C.3 CMS v1.0—Train record 83
- C.4 CMS v1.1—Train record 84
- C.5 CMS v1.1—Monitoring scheduler 85
- C.6 Antenna test 87
- C.7 Coverage test: gateway 89
- C.8 Coverage test: wireless sensors 91
- C.9 Measurements in Denmark (1) 93
- C.10 Measurements in Denmark (2) 94

C.11 Measurements in Denmark (3)	95
C.12 Measurements in Germany (1)	97
C.13 Measurements in Germany (2)	99
C.14 Measurements in Norway (1)	101
C.15 Measurements in Norway (2)	102
C.16 Measurements in Norway (3)	103

List of tables

3.1	Selected inertial sensors	12
3.2	Power consumption of wireless sensor (bypassed FIFO)	18
5.1	Node and coordinator RSSI for a certain distance	32

List of abbreviations

ADC analog-to-digital converter. 33, 34

ADI Analog Devices, Inc.. 11, 33, 34

API application programming interface. 20

BW bandwidth. 12, 33, 34

CDC Communication Device Class. 25

CMS content management system. 3, 20, 25, 26, 30, 31, 33

DESTination RAIL Decision Support Tool for Rail Infrastructure Managers. xvi, 1, 3, 30

ECTS European Credit Transfer and Accumulation System. iii

EEPROM electrically erasable programmable read-only memory. 15, 24

EMT equipped measurement trains. 8, 36

ERP effective radiated power. 26, 31, 32

ERTMS European Rail Traffic Management System. 20, 37

EU European Union. xvi, 1

FEM front end module. 26, 32

FFT fast Fourier transform. 34

FIFO first-in-first-out. 11–13, 34, 35

FW firmware. 14, 15, 19

GFSK Gaussian frequency-shift keying. 14

GPRS General Packet Radio Service. 30

GSM Global System for Mobile Communications. 30, 31

- GW** gateway. 20, 31–33, 91
- HI2OT** Nordic University Hub on Industrial Internet of Things. xvi, xvii
- HW** hardware. 12, 15–17, 19
- I²C** Inter-Integrated Circuit. 13, 16
- IBM** Department of Civil and Environmental Engineering. xvi
- IM** infrastructure manager. 1, 2, 22
- ISM** industrial, scientific and medical. 14
- ITK** Department of Engineering Cybernetics. xvi
- LPWAN** low-power wide-area network. iii
- LSB** least significant bit. 12, 13
- MEMS** micro-electromechanical systems. 3, 11, 36, 37
- MSB** most significant bit. 25
- MTP** Department of Mechanical and Industrial Engineering. xvi
- NTNU** Norwegian University of Science and Technology. xvi, xvii, 2
- ODR** output data rate. 13, 14, 33–35
- OS** operating system. 13–15, 24
- PCB** printed circuit board. 12, 14, 23, 31, 33, 79, 81
- PhD** Doctor of Philosophy. xvi, xvii, 4
- RCF** rolling contact fatigue. 6, 8
- RF** radio frequencies. 14, 15, 18, 19, 23, 24, 28, 30–32
- RFID** radio-frequency identification. 2
- RMS** root mean square. 13, 34
- RSSI** received signal strength indicator. 24, 32
- SIL** safety integrity level. 23, 36
- SIRI** Service Interface for Real-time Information. 3, 26, 37
- SMT** surface-mount technology. 14
- SPI** Serial Peripheral Interface. 15, 24, 25

SRAM static random-access memory. 15, 23, 24

SW software. 20

TUM Technical University of Munich. xvii, 2

USB Universal Serial Bus. 25, 28

WP work package. 2

WS wireless sensor. 11, 31–33, 75, 79, 81, 91, 95

WSC wireless sensor's casing. 19, 31–33, 79, 81, 102

WSN wireless sensor network. iii, 3

Preface

This thesis is submitted in partial fulfilment of the requirements for the degree of Doctor of Philosophy (PhD) at the Norwegian University of Science and Technology (NTNU).

The work presented in this thesis resulted from my previous work on the DESTination RAIL project, described in Section 1.1 and carried out at the Department of Civil and Environmental Engineering (IBM) from 09.2015 to 09.2017, and from work on my PhD project conducted at the Department of Mechanical and Industrial Engineering (MTP) from 10.2017 to 01.2021. My main supervisor was Professor Amund Skavhaug (MTP, NTNU) and my co-supervisors were Professor Mary Ann Lundteigen (MTP/ITK, NTNU) and Professor Stig Petersen (MTP, NTNU and SINTEF Digital).

This PhD project was part of the New Instruments for Nordic University Cooperation and has been supported by NordForsk funds under the Nordic University Hubs initiative. During my PhD studies I thus had the privilege of attending several summer schools, training days and meetings run by the Nordic University Hub on Industrial Internet of Things (HI2OT). I am grateful for all the presentations, lectures, training days and meetings, which were very enlightening and motivating, and connected me with researchers working on a similar or identical topics across Scandinavia. This had a strong positive effect on my work and the results presented in this doctoral thesis.

The parts of the Chapters 3 to 5 are a revised and extended version of the text delivered to the European Union (EU) in a deliverable report on the DESTination RAIL project Task 1.3: Monitoring of Switches, Crossings and Tracks [1]. I am the author of all the reused and revised text included here.

Acknowledgements

My greatest gratitude goes to Professor Amund Skavhaug for his supervision and for giving me the opportunity to pursue this doctoral degree at NTNU. Amund's faith in me and continuous support helped me to move forward even at times when the world around me was not so bright. This helped me to stay motivated and focus on what mattered. Next, I thank my co-supervisors Professor Mary Ann Lundteigen and Professor Stig Petersen for their valuable discussion and suggestions, especially at the beginning of my project and as we worked on the conference paper focusing on functional safety.

I also thank the academic and administrative personnel who contributed to the project. This work covers numerous topics and often required external expertise, which I was able to access promptly from kind and very enthusiastic staff: thanks for these valuable discussions. I also frequently needed to borrow or purchase equipment, which usually took me a lot more time and effort than I would ever have expected. I thank all those who helped me with these tasks, as this was challenging activity for all involved.

Sincere thanks to Bane NOR, Bane DK and DB Netz AG for allowing us to install, measure and collect data on their infrastructure. This required a lot of effort and organisation to receive all the clearance necessary, and a certain amount of manpower to make sure that all the tasks were performed in a safe and timely manner. Special thanks to Bane NOR, who agreed and allowed to release the collected data as an accessible dataset that can serve researchers around the world in their work. I also want to highlight and acknowledge Dr.-Ing. Bernhard Lechner and his PhD student Kangle Chen, both at the Technical University of Munich (TUM), for their help with the organisation and measurements in Germany. This field test would not have been possible without them, and I thank them for their effort, contacts and contribution to this project.

I thank all my colleagues at NTNU and the HI2OT framework for a great time, many fruitful discussions, and the many non-work related activities we enjoyed. I will always remember those great weekends spent in the Norwegian mountains.

Last, but not least, thanks to my family. Your continued support throughout my life eventually led me to this doctoral study and contributed to its successful completion. Even far from home I never felt really alone, as I always had you just one conference call away. You were always there for me, and I will always be there for you!

Chapter 1

Introduction

The implementation of Industry 4.0 poses many challenges and has implications for diverse fields that must keep up with innovations to allow this transition. For example, smart factories are highly dependent on logistics, which in turn requires predictive, reliable and highly functional transportation systems. Unreliable transportation causes problems for workers commuting to the factory and delays the delivery of goods and materials, eventually negatively affecting subsequent processes. Therefore all systems must work optimally to achieve the effectiveness required across complex processes.

This thesis seeks to contribute to such effectiveness by seeking ways to make interconnected transportation systems more reliable and robust in the face of unpredictable events. Specifically, it focuses on improving on current methods of railway turnout inspection, which has been an unresolved issue for several decades. While the inspection of most railway components has become more effective over time and is nowadays maintained relatively optimally, not much has changed in the inspection of railway turnouts. Due to the vast number of these parts in the railway infrastructure and their crucial role, even a small improvement here would have a significant social-economical impact, and it is therefore of major interest to infrastructure managers (IMs). Therefore this thesis proposes inspecting railway turnouts via remote monitoring using low-cost inertial track-side sensors that were built and demonstrated during this doctoral study.

A substantial amount of this thesis is based on my previous work on the DESTination RAIL project. This was an European initiative of several railway administrations, research institutes and universities across Europe to resolve the biggest deficiencies in the railway industry. The whole project, whose abbreviation stands for Decision Support Tool for Rail Infrastructure Managers, was supported by the EU Research and Innovation programme Horizon 2020 to the tune of 3 million euro, with an overall budget of 3.9 million euro. My contribution to this project was in Task 1.3—Monitoring of Switches, Crossings and Tracks. The official description of this task is quoted in Section 1.1, and the outcomes of my work on this project are documented in the EU deliverable report [1].

1.1 DESTination RAIL Project

Task 1.3—Monitoring of Switches, Crossings and Tracks

Monitoring the condition of switch and crossings is a challenge for infrastructure managers. It requires specially trained switch inspectors to manually check the condition of the track. Existing tools to monitor the geometric quality of the track are not fully applicable to switches and crossings. Further track stiffness monitoring vehicles cannot monitor these critical rail infrastructures. Hence, a fast and cheap system to continuously monitor the Switches and Crossings is a crucial matter for railway IMs. This project aims to develop a methodology to continuously monitor critical track infrastructures, such as switches and crossings, using inbuilt sensor technologies. The sensor will communicate with passing trains/monitoring trains to inform the status and condition of the switch in conjunction with WP2. NTNU and TUM will use the simulation tool developed to select suitable data acquisition components and integrate these into the chosen architecture (Sensors, Communication - wired and possibly wireless depending on sensor location). They will develop and install a data analysis and storage system, and communication system to transfer data in real time and mount the sensors in track infrastructure that can communicate with a train and test the system in lab environment. Demonstrate the inbuilt technology at a test site in Norway. Monitoring of track condition is performed by all IM's using instrumented trains. To maximize efficiency of the modeling tools applied by TUM in WP2 accurate referencing of such train borne data to the respective rail seats along the track (microscopic train-track-substructure modeling) is needed. However, this data is typically not provided by the measurement trains, e.g. using measurement train data for evaluation of track quality degradation requires synchronization of the data according to track location first. Two different approaches will be studied by TUM:

- Methods to improve track recording train data analysis of actual measurement procedures to achieve highest accuracy concerning accurate rail seat referencing and to gain this data as input for modeling work or for model calibration.
- Possibilities to improve data sampling of measurement trains with regard to accurate rail seat referencing of such vehicle borne data (e.g. using the RFID technique).

Abbreviations: work package (WP2); radio-frequency identification (RFID)

1.2 Research Objectives

- Resolve known deficiencies of the DESTination RAIL WSN.
- Manufacture 30 wireless sensors and 3 gateways.
- Build CMS¹ on Drupal 9, implement SIRI², prepare RailCheck dataset distribution.
- Obtain Bane NOR's approval to deploy the system and create accessible dataset.
- Deploy system on railway turnout in Norway.
- Collect a year's worth of data from the RailCheck system.
- Briefly process the data and propose algorithms that identify faulty states.
- Sanitise the data and release them as RailCheck dataset for academic/research use.
- Publish two conference papers and one journal paper.

1.3 Scope

The transition from preventive to predictive maintenance can be summarised as below to describe the steps required to achieve the desired state:

- See—What is happening?
- Understand—Why is it happening?
- Prepare—What will happen?
- Adapt autonomous—Perform autonomous action!

Due to the complexity of this project and the time limitation of the doctoral study, this thesis deals only with the first item on the list—'See'. Therefore the majority of this work focuses on the creation of a functional measuring system for use in real traffic today rather than on analysing the data, which have been released as an accessible dataset. The main questions to be answered are:

- Can low-cost inertial MEMS³ sensors provide sufficient data for further analysis?
- Is the concept itself viable in terms of functionality, cost and power consumption?
- Can the system be certified and used in real traffic today?
- Can the system be reliable, maintenance-free and user-friendly?
- What are the parameters and limitations of this system and are they acceptable?

The measurements are intended to be performed on a railway turnout; and a nominal track or any other construction or its parts are excluded from this examination.

¹content management system

²Service Interface for Real-time Information

³micro-electromechanical systems

1.4 Motivation

We are approaching a time when we will be technologically capable of gathering high-quality vehicle-track interaction data at no additional cost compared to today, but we will not have reliable algorithms with which to process them. This will pose a major challenge for the transition from preventive to predictive maintenance in the not-so-distant future. Creating accessible datasets is a first step in supporting research in this area.

1.5 Contributions

The main contributions of this thesis are as follows:

- Sensory system designed, built and verified in laboratory setting.
- System deployed and validated on rails in Denmark, Germany and Norway.
- Deficiencies removed and system deployed as a permanent test bed in Oslo tunnel.
- A year's-worth of data collected and made available for academic and research use.
- Information about the proposed sensory system disclosed.
- Data briefly analysed to demonstrate the potential of the dataset.
- Functional safety study to ascertain whether the system can be certified for use.
- ADXL372 misalignment bug identified, reported and made recognised.

1.6 Publications

The PhD project produced two published conference papers and a journal paper. These are listed below and are attached in Section A.

Conference Papers

- J. Sramota and A. Skavhaug, "RailCheck: A WSN-Based System for Condition Monitoring of Railway Infrastructure," 2018 21st Euromicro Conference on Digital System Design (DSD), Prague, 2018, pp. 347-351, doi: 10.1109/DSD.2018.00067.[2]
- J. Sramota, M. A. Lundteigen, S. Petersen and A. Skavhaug, "RailCheck: Functional Safety for Wireless Condition Monitoring of Railway Turnouts and Level Crossings," 2019 IEEE Intelligent Transportation Systems Conference (ITSC), Auckland, New Zealand, 2019, pp. 3188-3193, doi: 10.1109/ITSC.2019.8917093. [3]

Journal Paper

- J. Sramota and A. Skavhaug, "RailCheck Dataset of Vehicle-Track Interaction Measured on Railway Turnouts,"[4]
Note—The journal paper submitted and waiting for review.

Chapter 2

Background

2.1 Rail Defects

This chapter is based on the book [5] and the track engineering manuals [6, 7], and provides a quick overview of some of the most common railway track defects. The following Section 2.2 then provides information about the usual ways of resolving these.

2.1.1 Rolling Contact Fatigue Defects

Rolling contact fatigue (RCF) defects are failures driven by crack propagation near the rail surface due to an alternating stress field. They are generic in nature and are caused by excessive shear stress at the wheel-rail contact interface. These defects can be observed on sharper curves and are considered the least avoidable failure in rolling contacts.

The **gauge corner** checking shown in Fig. 2.1a are cracks initiated at or close to a running surface occurring at 2 to 5 mm intervals and growing to 2 to 5 mm in depth. They gradually spread across the rail-head and break off as small wedges or spalls.

The **shelling** defects shown in Fig. 2.1b do not form as often as gauge corner defects. They develop on a horizontal or longitudinal plane and grow in the direction of train travel. They either spall out into a shell or turn downwards and form a **transverse** defect that, if undetected, continues to grow and can lead to rail failure. The transverse defects shown in Fig. 2.1d cannot be detected visually and rely on ultrasonic inspection.

With **running surface** checking, also called **flanking**, defects initially appear in a mosaic or snakeskin-like pattern on a running surface. Later these cracks produce spalls of up to 10 to 15 mm wide and 3 mm deep, as shown in Fig. 2.1c.

2.1.2 Other Defects

The rail **corrugations** shown in Fig. 2.1e are the result of vertical cyclic wear that develops from wheel-rail contact over time, creating irregularities on the running surface that

can be categorised by pitch to short or long. Short pitch corrugations have a wavelength of 30 to 90 mm with a depth of 0.2 to 0.3 mm, and are often formed by lighter nominal axle loads of up to 20 tons. Long-pitch corrugations have a wavelength of over 300 mm and can reach over 2 mm deep as a result of higher nominal axle loads of over 20 tons.

Squats are subsurface laminations that initiate at small cracks and grow diagonally downwards until they reach 4 to 6 mm in depth, and then spread laterally and longitudinally on the running surface. Squats develop gradually over a period of months or years, and tend to occur on tangent track and curves with a radius of 800 to 1600 metres, as shown in Fig. 2.1f. Squats can be initiated by wheel slip damage among others.

The **wheel or engine burns** shown in Fig. 2.1g are similar to small squats; however, they always appear suddenly and in pairs directly opposite one another on both rails. They are caused by the locomotive drive wheels slipping on the rails during acceleration. Wheel burns can be more than 50 mm in length, or substantially longer if the locomotive is already in motion when the wheels slip due to insufficient traction.

Tache ovales or **shatter cracks**, also known as **transverse fissures**, are internal defects caused by the presence of excessive hydrogen in rail steel or welds. These defects and their development are similar to those of the transverse defects shown in Fig. 2.1d, the difference being that the source of the defect is not the gauge corner but is somewhere within the rail-head and is initiated at much greater depths. Improvements in manufacturing processes and ultrasonic inspection have greatly reduced this risk.

The **vertical or horizontal split head** defects shown in Fig. 2.1h are separations in the rail-head that tend to split it into two parts. Medium and large defects can be observed visually, but the initial stage can only be detected ultrasonically.

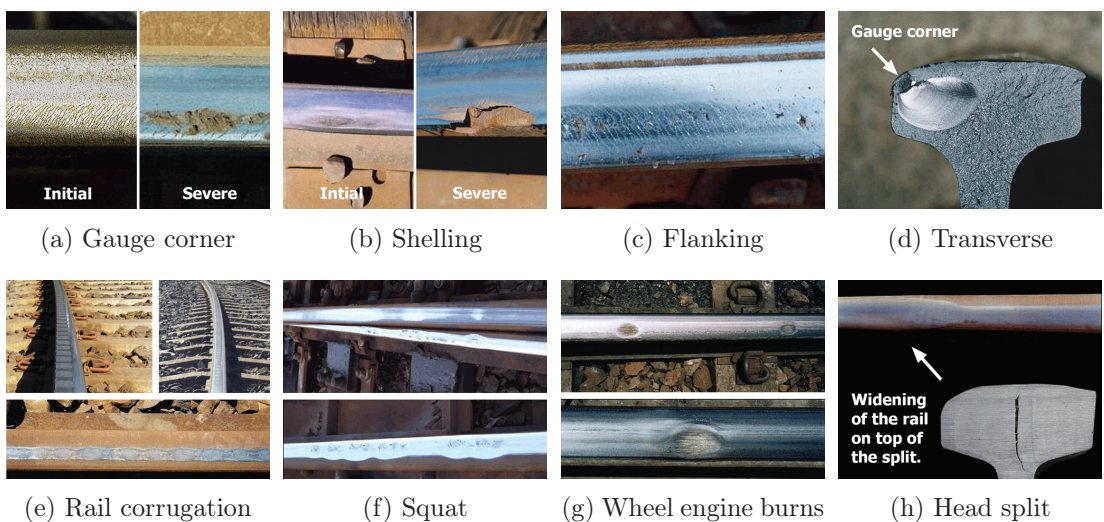


Figure 2.1: Rail defects

2.2 Rail Maintenance

Effective maintenance is an essential element to ensure safe and efficient transportation. Nominal tracks are regularly inspected by equipped measurement trains (EMT) using cameras and laser-based systems. Railway turnouts, on the other hand, are predominantly inspected manually as EMT are not well-suited to making such measurements, as described in Paper A.3. This makes railway maintenance more expensive than necessary.

Rail service life is primarily determined by wear, plastic flow and defects. The wear usually occurs on the gauge face due to high wheel-flanging forces, e.g. on curves, turnouts and running surfaces, and is caused by wheel-rail interaction and maintenance activity as it is grinding. Plastic flow is experienced when contact stresses at the wheel-rail interface exceed the strength of the material. This leads to rail corrugation and squat development. Rail defects can occur for many reasons and are a major concern. If undetected, they can eventually require expensive maintenance or can even cause rail failure.

Due to the various improvements that have reduced the rail wear and thus prolonged their life, the occurrence of defects has generally increased [6]. RCF defects moreover do not develop uniformly, and their progress accelerates throughout the rail's life. They can only be observed visually about three quarters of the way through the rail's life and are therefore hard to detect or predict early on using visual methods. Furthermore, the life of a railway turnout varies from 27 to 100 Mt, making optimal periodic maintenance intervals hard to set to cover rails with short, mean, and long lives [8].

2.2.1 Rail Grinding

High tractive forces and the sheer weight of trains make the hard surface of rails brittle over time, leading to damage from rolling contact fatigue and the creation of micro cracks or worse—head checks. Grinding to remove the top 2 mm layer of the rail material early on eliminates cracks so they cannot grow and removes rail irregularities that would otherwise lead to excessive dynamic forces, and preserves the track in a good operational state. The process of grinding the rails is shown in Fig. 2.2a.



(a) Rail grinding

(b) Rail tamping

Figure 2.2: Rail maintenance

2.2.2 Rail Tamping

Rail transport generates strong dynamic forces whose continued stresses can cause a track to deviate from its ideal position. If this deviation becomes excessive, the track must be tamped to correct the vertical and lateral axes of the track geometry and adjusted for cant excess or deficiency. The rails are lifted and repositioned, and the tamping machine drives vibrating tines into the ballast at 35 Hz until squeezing depth is achieved, as shown in Fig. 2.2b. This figure shows the horizontal wheel positioned close to the rail-web used for hoisting the rail. The machine operator thus must avoid existing installations in this area.

2.2.3 Rail Replacement

The decision to replace rails is always a last resort due to the high cost involved. However, on some highly loaded tracks the rails and turnouts are replaced every few years, especially where the track includes highly loaded curves, turnouts, and uphill sections. Otherwise tracks last for several decades in the vast majority of cases, depending on the traffic and the loads they support. Regular maintenance plays a significant role here.

Chapter 3

Analysis

The majority of stationary track-side railway measurements today are realised using industrial sensors that are expensive and require a wired connection to power the device and exchange data. While these sensors provide highly accurate measurements, they are inherently not well suited for permanent or mass-scale installations. The proposed system aims to resolve these drawbacks and provide an affordable solution for extensive installations that can be easily deployed and operated and require minimum maintenance. The goal of this project is to discover whether systems such as this can deliver sufficient data for condition-based maintenance and contribute to further progress in this area.

The RailCheck system shown in Fig. 3.1 consists of wireless sensors, a gateway and a server. The wireless sensors, which attach to the rails, comprise a digital inertial sensor, a battery and a communication module, and sense vibration from overpassing trains. When required they can record vehicle-track interaction and send the data wirelessly to the nearby gateway, which forwards them to the server for aggregation, analysis and storage. The relevant vehicles receive information about identified track defects immediately through direct communication channels, or indirectly through programmable balises or other railway infrastructure. The strong integration with existing communication networks and surrounding infrastructure result in low overall deployment, operation and maintenance costs, and contributes to the smoother adoption of this system.



Figure 3.1: Proposed concept

3.1 Wireless Sensor

The wireless sensor (WS) is a small electronic device attached to the field side of the rail, therefore to the opposite side of the gauge face and the vehicle's wheel-flange, as demonstrated in Fig. 3.3b. It consists of electronic components that record forces experienced during vehicle-track interaction and forward the resulting data wirelessly to the server. Each wireless sensor is powered by its own battery for its lifetime, and its low-power consumption is therefore the main point of interest. The wireless sensor must be durable, reliable, affordable, compact in size, maintenance-free and easy to install and operate.

3.1.1 Sensors

Each wireless sensor is equipped with a digital inertial sensor based on MEMS technology and a digital temperature sensor. Information about local temperature at the measuring point is used to supplement the acceleration data with additional information for further analysis. The MEMS acceleration sensor is used for its favourable attributes compared to a legacy inertial sensors. MEMS sensors are usually small in size ($\approx 5 \text{ mm}^2$), negligible weight ($\approx 50 \text{ mg}$), with low-power consumption ($50 \mu\text{A}$ per axis sampling at 3200 Hz) and low-cost (at a few dollars per unit), and are robust and reliable (tolerating shocks over 10,000 g, AEC-Q100 certified, stable over time and temperature). On the other hand, the MEMS inertial sensors are restricted to applications that can tolerate lower bandwidths with greater noise, while diagnostic applications require less noise at higher frequency ranges beyond 10 kHz. MEMS acceleration sensors currently offer just few dozen kHz with noise density levels anywhere from 1 to 1000 $\mu\text{g}/\sqrt{\text{Hz}}$. Putting aside the performance factor, there are many reasons why MEMS sensors are often considered for condition-based monitoring, as they enable applications that would not be viable.

Analog Devices, Inc. (ADI), currently the biggest manufacturer of consumer-grade multipurpose accelerometers, was selected as the main supplier for this project. Its digital MEMS accelerometers are often fitted with advanced built-in logic that contributes to low-power consumption. For example, their low-g threshold activity and inactivity detection enables them to detect acceleration above and below user-set thresholds. In addition, the user can set activity and inactivity timers that restrict the reporting of activity and inactivity events unless sustained motion is recognised. This and other features, such as filters and absolute and referenced thresholds, allow flexible motion detection with sampling rates of units up to dozens of Hz at very low-power. The acceleration sensor can be set to continuously measure the presence or absence of motion and respond to these events automatically in several ways, one of which is by setting up the interrupt pin to wake up downstream circuitry. This function is used to detect incoming trains and sense their presence while keeping the power consumption to a minimum. Another useful feature that contributes to low-power use is a first-in-first-out (FIFO) buffer which release the host processor to attend to other tasks or to sleep for extended periods.

The principle of the accelerometer’s operation in this project is as follows. In wake-up mode the digital accelerometer continuously monitors vibrations on the rail, and once these exceed the level set, indicating an oncoming train, the sensor wakes the rest of the electronics. The woken microcontroller then switches the accelerometer to full measurement mode and records vehicle-track interaction. Once the level of acceleration drops below the threshold specified, the train is gone and the accelerometer indicates inactivity. The microcontroller sets accelerometer to standby, forwards data to the gateway and sets the accelerometer back to wake-up mode and sends the rest of the electronics back to sleep. Because of this routine means the accelerometer spends most of its time in wake-up mode waiting for oncoming trains, very low-power consumption in this mode is crucial.

When a train passes over the sensor with a sampling rate set to 3200 Hz at a velocity of 160 km per hour, the acceleration sensor samples for every 13.9 mm of the length of the train (Eq. 3.1). Considering the wheel size, the peaks of deflection should be sufficiently recorded when the train axles are above the sensor, as demonstrated by Chraim [9].

The accelerometer ADXL313 was selected based on the requirements outlined above and information provided by Chraim [9]. The sensor samples up to 3200 Hz, and has a high sensitivity of 1 mg per least significant bit (LSB) and low noise density of 150 $\mu\text{g}/\sqrt{\text{Hz}}$. At the same time it measures a very narrow range of ± 4 g, which can be limiting. It is expected that sensed acceleration might be out of range and therefore insufficient for the given measurements which would end up saturated. In such a case it is possible to replace the sensor with an alternative, as shown in Table 3.1. The printed circuit board (PCB) layout could be preserved in the case of the ADXL312 (± 12 g), but would have to be revised for use with the ADXL345 (± 16 g) or ADXL375 (± 200 g).

$$l_{\text{sample}} = v \cdot T = \frac{160 \cdot 10^3}{60^2} \cdot \frac{1}{3200} = 13.9 \text{ mm} \tag{3.1}$$

Table 3.1: Selected inertial sensors

HW	Type	RNG	BW	SEN	NOI	CON	FIFO	Launched
1.0	ADXL313	± 4	1600	1.0	150–250	55–170	32	2013-05
1.1	ADXL343	± 16	1600	3.9	290–430	45–140	32	2012-03
1.1	ADXL372	± 200	3200	100	5300	3.6–22	169	2017-03
—	ADXL312	± 12	1600	2.9	340–470	55–170	32	2009-10
—	ADXL345	± 16	1600	3.9	290–430	45–140	32	2008-11
—	ADXL375	± 200	1600	49	5000	40–145	32	2013-06

Legend: HW—used in PCB version; RNG—Range [g]; BW—Bandwidth [Hz]; SEN—Sensitivity [mg/LSB]; NOI—Noise $xy-z$ [$\mu\text{g}/\sqrt{\text{Hz}}$]; CON—Consumption, wake-up–measurement mode [μA]; FIFO—First-in-first-out buffer [depth levels];

Sensors used in HW design:

Thermometer—Microchip Technology MCP9808

Microchip MCP9808 is a digital sensor that converts temperatures from -40°C to $+125^{\circ}\text{C}$ to a digital word sent by Inter-Integrated Circuit (I^2C) with a maximum accuracy of $\pm 1^{\circ}\text{C}$ (typ. $\pm 0.25^{\circ}\text{C}$). The maximum accuracy for the range of -20°C to $+100^{\circ}\text{C}$ is $\pm 0.5^{\circ}\text{C}$ (typ. $\pm 0.25^{\circ}\text{C}$). The typical operating current is $200\ \mu\text{A}$, and the shutdown current is up to $100\ \text{nA}$. This sensor is fitted in many IQRF modules except the one used in this project and is directly supported by the IQRF operating system (OS). If it is connected to the same pins as the OS expects, the sensor can be used without additional programming.

Accelerometer—Analog Devices ADXL313 (PCB v1.0)

The ADXL313 measures excitation at up to $\pm 4\ \text{g}$ with a sensitivity of $1\ \text{mg}$ and root mean square (RMS) noise of $1.5\ \text{LSB}$. The output data rate (ODR) can be set to up to $3200\ \text{Hz}$ with a power consumption of $170\ \mu\text{A}$. In wake-up mode the ADXL313 can sample 12.5 times per second with a consumption rate of $43\ \mu\text{A}$. The accelerometer is fitted with a 32-level multi-mode FIFO buffer that allows it to store up to $10\ \text{ms}$ of data.

Accelerometer—Analog Devices ADXL343 (PCB v1.1)

The ADXL343 was designed as a versatile accelerometer with a magnitude of up to $\pm 16\ \text{g}$ and a sensitivity of $3.9\ \text{mg}$ with RMS noise of $1.1\ \text{LSB}$. It is equipped with 32-level FIFO and consumes $140\ \mu\text{A}$ at ODR $3200\ \text{Hz}$ and about $30\ \mu\text{A}$ in wake-up mode, with a sampling rate of 8 times per second. This sensor lacks the external clock feature.

Accelerometer—Analog Devices ADXL372 (PCB v1.1)

The ADXL372 was designed as a multi-purpose accelerometer with a range of up to $\pm 200\ \text{g}$ for high-g impact and shock detection and it is equipped with functions that are useful for condition-based assessment. The ADXL372 is fitted with 4-pole low-pass anti-aliasing filter to attenuate out the band of signals that are common in high-g applications. It also incorporates a high-pass filter that eliminates initial and slow-changing errors such as ambient temperature drift. The 12-bit resolution provides a sensitivity of $100\ \text{mg}/\text{LSB}$ with RMS noise of $3.5\ \text{LSB}$. The ODR can be set to up to $6.4\ \text{kHz}$ and data can be stored in 169-level deep FIFO that can hold $80\ \text{ms}$ of three-axial data at maximum sampling frequency. The power consumption in wake-up mode, with sampling at 19 times per second, is $\approx 5.8\ \mu\text{A}$ (wake-up timer— $52\ \text{ms}$, filter settling time— $16\ \text{ms}$). The sensor can utilise an external clock to resolve the time base instability described in Paper [A.3](#).

3.1.2 Communication

Wireless communication refers to the transmission of information between at least two subjects without wires, cables or any other form of electrical connection. As part of this project the carrier medium will be radio frequencies (RF) with a communication distance of up to a few hundred meters. Each sensor is expected to generate up to 192 kB of data per train passing. This value is calculated based on the ODR of the accelerometer sensor sampling 3 axes at 3.2 kHz for duration of 10 seconds. During this time a train travelling at a velocity of 160 kmh^{-1} will pass over 450 meters of rails. Since the average train in Norway is 75 to 150 meters long, the 10 seconds measuring window should provide a sufficient time-frame for measuring even slower vehicles and the sampling rate can be further adjusted to lower frequencies more appropriate for vehicles moving slowly.

Data need to be transmitted from the sensors on a rail-body to a nearby gateway up to a few hundred meters away. The chosen solution must be reliable, affordable, and power-efficient to sustain many years of battery operation. The most suitable solution is to use low-power RF modules that perform well in given environments, are very compact and can easily be embedded in a custom design. Many products implement various protocols such as Wi-Fi, ZigBee, BLE, UWB, LoRa and IQRF. With so many different standards and protocols it is not easy to find a balanced solution, especially for battery-powered application. After comparing the positives and negatives, especially regarding the power consumption requirements, the IQRF platform was chosen as most suitable for the task.

RF Module—IQRF TR-76D

The IQRF TR-76D [10] is an affordable RF module which costs around 8.5 dollars for quantities of 1k+ and can be easily integrated into other PCB designs using surface-mount technology (SMT). It communicates on industrial, scientific and medical (ISM) wavebands at 868 MHz with Gaussian frequency-shift keying (GFSK) modulation at data rates of up to 19.836 kbps. Higher data rates of up to 500 kbps can be achieved by implementation of custom routines into one of the firmware (FW) revisions. The very low-power consumption (TX 8.3 to 25 mA, STD RX 11.8 mA, LP RX 250 μA , XLP RX 16.3 μA), -101 dBm RF sensitivity, 10 mW RF output power, wide communication range of $500^1/1100^2$ metres, and small size at just 15.2 x 14.9 x 3.3 mm makes this module an optimal solution. The module is fully controlled by the user application program, where developers may use some of the inbuilt functions of the OS to accelerate its development. The IQRF ecosystem also integrates easily with other IQRF devices such as gateways and the Cloud, as described in Sections 3.2 and 3.3.

¹2x TR-76DA plugged in DK-EVAL-04A vertically 1.6 m above ground, reflective planes >100 m

²same as in ¹, just TR-76DA plugged in DK-EVAL-04A through RNG-EXT-01 adapters

3.1.3 Memory and Processing

Processing—IQRF TR-76D

The RF module IQRF TR-76D utilises a Microchip PIC16LF1938 for its internal operation to which users can upload their custom FW. The user application then runs most of the time, interrupted only for short periods by the OS when the module has to service RF routines. Using the TR-76D both for communication and as a microcontroller for all other tasks contributes to the wireless sensor's lower cost and power consumption.

Memory—Microchip 23LC512

The digital accelerometer ADXL313 produces 3200 samples per second, each with 13 bits in full resolution mode, on each of three axes. Unless data compression is used, the sensor collects 192 kB of data in 10 seconds, which must be stored before they can be pre-processed and transmitted further. The static random-access memory (SRAM) was selected against the electrically erasable programmable read-only memory (EEPROM) due to its unlimited writing and reading cycles, zero waiting time, and power efficiency. Due to its many benefits the Microchip SRAM was selected for use in the wireless sensor. The supplier offers various capacities with the same layout at reasonable prices.

Microchip 23LC512 is a serial SRAM with 512 kbit capacity and the Serial Peripheral Interface (SPI) operating at up to 20 MHz. The operating current is typically 1 mA (max. 10 mA) and the standby current is about 1 μ A (max. 4 μ A). Data are organised in 64k x 8-bit cells and are accessible as bytes, pages or sequences. The memory has zero write time and supports unlimited reads and writes to the memory array. Operational temperature range is -40°C to +85°C. If bigger SRAM were ever needed, the 23LC1024 doubles the memory space and uses the same layout, thus not requiring hardware (HW) revision.

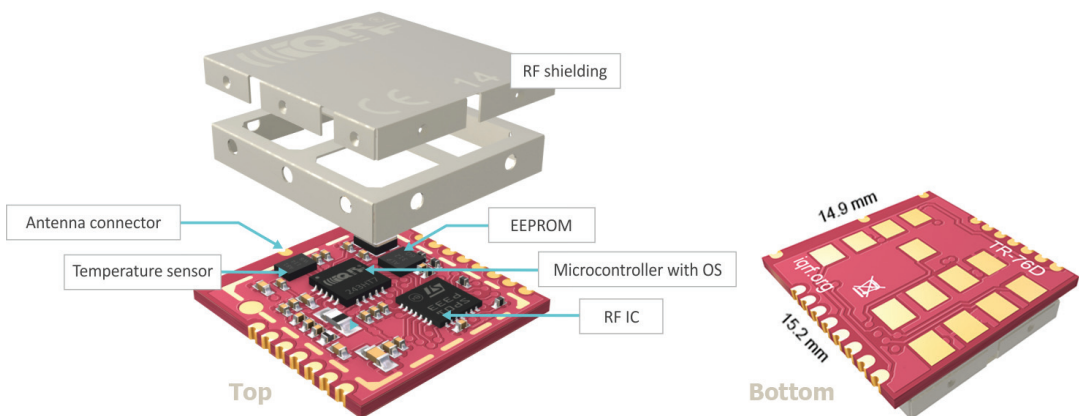


Figure 3.2: IQRF TR-76D

3.1.4 Power Management

For applications lasting from many years to decades a special type of battery is required since most conventional batteries self-discharge after a while, even when not in use. To overcome this, the lithium-thionyl chloride (Li-SOCl₂) cell is used as a power source. This battery is well-suited to demanding extremely low-current applications where long life is essential. The cell offers high energy density, a wide operating temperature range and a stable nominal voltage of 3.6 V for most of its operational life. The buck-boost DC/DC converter was added to deliver stable voltage in all conditions.

Battery—Saft LS26500

The Saft LS26500 battery is a primary lithium-thionyl chloride C-size bobbin cell designed for applications with a lifespan of more than ten years. It has a very low self-discharge rate of less than a 1% after 1 year of storage at +20°C, superior resistance to atmospheric corrosion, a wide operating temperature range of -60°C to +85°C and high voltage response stable during most of its operational life. The nominal capacity is stated as 7.7 Ah, which corresponds to 27.72 Wh, and the cell weight is just 48 grams. The nominal voltage of 3.6 V can however drop below 3 V in temperatures below -10°C, when the battery loses its ability to deliver higher continuous currents over 30 mA.

DC/DC Converter—Linear Technology LTC3335

The Linear Technology LTC3335 can compensate for this battery voltage drop as it stabilises the operational voltage across various temperatures. This is done using a high-efficiency nanopower buck-boost DC/DC converter specifically designed for long-term battery-powered applications. The converter delivers output voltage that is either greater or lower than the input voltage, and therefore the sensor will still work in very cold weather when the battery cell voltage drops below the selected three volts. Output voltage can be set to [1.8, 2.5, 2.8, 3, 3.3, 3.6, 4.5 or 5] volts using external components, or changed dynamically over the I²C interface. The programmable peak input current, [5, 10, 15, 25, 50, 100, 150 or 250] mA, which enables the battery to discharge in a very controlled way, prolonging its lifespan, is a useful feature. The converter is up to 90% efficient using extremely low currents, e.g. its low input quiescent current at output voltage in regulation at no load is only 680 nA. Its integrated coulomb counter is another beneficial feature for continuous and precise monitoring of how much energy has been consumed.

The LTC3335 requires passive components to determine its properties. Selected values for HW design and some of the most important calculations are shown on the next page. Eq. 3.2 shows the duration for which the output voltage is in regulation and the converter sleeps. This value ranges from 18.8 μ s to 28.8 ms based on the load current, which can be from 16.3 μ A to 25 mA. Eq. 3.2 values are counted for the DC sleep hysteresis window which is ± 10 mV for the $V_{OUT}=3$ V. The ceramic capacitors $C_{IN}=10$ μ F

and $C_{OUT}=47 \mu\text{F}$ are recommended for the calculations. In future revisions the output capacitor may be replaced by the higher-value low-leakage aluminium electrolytic capacitor or super capacitor. Eq. 3.3 calculates the maximum inductor value taking into account a typical $\pm 20\%$ manufacturing tolerance, using, however, the $L_{REC}=100 \mu\text{H}$. Eq. 3.4 and 3.5 calculates the ON and OFF time of the regulator H-Bridge. The t_{AC} must never exceed $11.47 \mu\text{s}$, above which its measurement of charge transferred from the battery is inaccurate. Coulomb counter errors and input quiescent current errors in Eq. 3.6 account for 0.077% of battery charge loss a year. Eq. 3.7 calculates the maximum current that can be delivered by the regulator with the actual settings.

Selected values for HW design

BAT	$= 3.6 \text{ V}$	nominal battery voltage (at 0.5 mA, $+20^\circ\text{C}$) minimum battery voltage (at 25 mA, -40°C) output regulated voltage (LTC3335 $V_{OUT}=V_{DD}=V_{AA}$) selected according to LS26500 datasheet
BAT_{MIN}	$= 2.75 \text{ V}$	
V_{OUT}	$= 3.0 \text{ V}$	
I_{PEAK}	$= 100 \text{ mA}$	

The duration for which regulator sleeps

$$t_{SLEEP} = C_{OUT} \frac{V_{DC_HYS}}{I_{LOAD}} = 47 \mu \frac{10\text{m}}{25\text{m}} = 18.8 \mu\text{s} \quad (3.2)$$

Inductor selection

$$L_{MAX} = \frac{0.8 \cdot BAT_{MIN} \cdot L_{REC}}{1.8} = \frac{0.8 \cdot 2.75 \cdot 100 \mu}{1.8} = 122.22 \mu\text{H} \quad (3.3)$$

Switching times of power FETs (H-Bridge)

$$t_{AC} = AC(ON) = \frac{I_{PEAK} \cdot L_{REC}}{BAT} = \frac{100\text{m} \cdot 100 \mu}{3.6} = 2.77 \mu\text{s} \quad (3.4)$$

$$t_{BD} = BD(ON) = \frac{I_{PEAK} \cdot L_{REC}}{V_{OUT}} = \frac{100\text{m} \cdot 100 \mu}{3} = 3.33 \mu\text{s} \quad (3.5)$$

Coulomb counter errors

$$q_{AC(ON)} = \frac{I_{PEAK} \cdot t_{AC}}{2} = \frac{100\text{m} \cdot 2.77 \mu}{2} = 138.5 \text{ nA} \quad (3.6)$$

Load current capability

$$I_{LOAD(MAX)} = \frac{I_{PEAK}}{2} \frac{BAT}{BAT + V_{OUT}} = \frac{100\text{m}}{2} \frac{3.6}{3.6 + 3} = 27.27 \text{ mA} \quad (3.7)$$

Power Consumption

The wireless sensor must have a very long operational life to be economically viable. Thanks to modern microcontrollers, power-efficient RF modules and battery types such as Li-SOCl₂ primary cells, the various applications may be powered for more than a decade depending on average power consumption, environmental conditions and the parameters of the battery cell, which can vary significantly from supplier to supplier.

While the power consumption of each electronic component used in wireless sensor design is known and the working conditions and average self-discharge rate of the battery can be estimated, actual power consumption will always vary widely. Some of the most significant factors are the amount of data to be transferred, changes in ambient temperature and the level of code optimisation. The calculations below offer at least a brief idea of expected power use, but actual estimates of expected lifespan must be gathered later from long-term measurement using the LTC3335 coulomb counter.

Selected Values

Measure a day	5	trains
Data per train	192	kB
RF data-rate	2.5	kBs
Sampling frequency	3200	Hz

Expected Values

Battery capacity	7700	mAh
Consumption per year	1305	mAh
Lifetime	5.9	years

Table 3.2: Power consumption of wireless sensor (bypassed FIFO)

Part	Mode	T [min]	Power consumption		
			AVG [μ A]	per Day [μ Ah]	per Year [mAh]
TR-76D	Sleep	0.0	0.06	0.0	0.0
ADXL313		1439.2	0.10	2.4	0.9
MCP9808		1440.0	0.10	2.4	0.9
LTC3335		1425.6	0.68	16.2	5.9
23LC512		1440.0	4.00	96.0	35.0
TR-76D	Operating	0.8	1600	22.2	8.1
ADXL313		0.8	170	2.4	0.9
23LC512		0.0	2000	0.0	0.0
MCP9808		0.0	200	0.1	0.1
LTC3335		14.4	360	86.4	31.5
TR-76D	RX XLP	1432.1	16.3	389.0	142.0
	TX STD	7.1	25000	2957.6	1079.5
			TOTAL:	3574.7	1304.8

Legend—**T**—Time; **AVG**—Average;

3.1.5 Mechanical Casing

The importance of the design of the wireless sensor’s casing (WSC) is easily underestimated in many similar projects. Designers often tend to focus on HW and FW parts, as one dysfunctional element in the communication chain can stop the entire system working. However, getting something such as simple as the casing wrong can cause serious trouble and significantly affect the performance of the whole system. Poor design can lead to:

- RF signal attenuation caused by e.g. inappropriate polarisation, location close to a ground or conductive planes, signal dispersion in inappropriate directions.
- Excessive mechanical stress, potentially causing e.g. casing disintegration, moisture or water ingress, damping or additional vibration, casing displacement.
- Physical damage to the casing e.g. by ballast stones, snow removal tools, maintenance activity or by deliberate action.

For these reasons the selection of materials used and the design and construction demand careful consideration. It is desirable that all components are located in one compact case.

Equally important is the positioning of the wireless sensor on the rail. A study by Cai [11] examined how acceleration varies according to the measuring points shown in Fig. 3.3a, and recommends the placement of the sensors on the rail-web at positions 3 to 5, where the acceleration values are relatively stable compared to other positions. Positions 1 and 2 on the gauge side of rail are excluded by the presence of a wheel-flange, and placement on the field side of the rail is highly discouraged as any equipment there is exposed to and in the way of snow removal tools and grinding and tamping machines. This disallows the use of the favourable vertical polarisation shown in Fig. 3.3b, which would be ideal as it would position the wireless sensor’s antenna as far from the ground and the rail’s conductive plane as possible for better signal propagation. Position 3 on the field side of the rail was finally selected as the optimal possibility for this application.

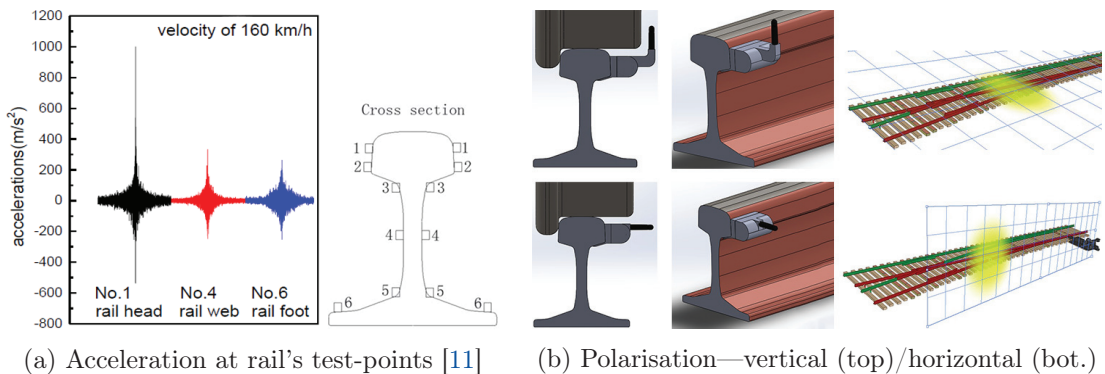


Figure 3.3: Installation of wireless sensor on a rail

3.2 Gateway (& Cloud)

The gateway (GW) forms a communication cell and controls communications with the surrounding wireless sensors. It is responsible for the wireless sensors' actions, for data consistency, and for forwarding the data and all supplementary information to the the IQRF Cloud. The connectivity between the gateway and the server is expected to be eventually realised using European Rail Traffic Management System (ERTMS) communication networks, but for now it makes use of public 4G networks. The aim is to use as many ready-made products as possible to speed development and focus on the important parts of the project. Therefore the full communication chain with use of IQRF gateway and IQRF Cloud, shown in Fig. 3.4, will be utilised to ease the realisation.

3.3 Server

Data from wireless sensors will be stored, analysed and delegated from the CMS shown in Fig. 3.4, the last element in the RailCheck system's communication chain. Authorised users will be able to access data on the Internet from anywhere via the HTTPS protocol. The CMS is needed because the IQRF Cloud only stores data in the format in which they arrive from the wireless sensors, so as a 64-byte-long packets, and its capacity is limited to a few thousand records. Working with data in such a format is impractical and complicated, and the data are erased at a certain moment. Therefore the data are regularly moved to the CMS server, where they are verified and assembled, enabling relevant information, including plotted train acceleration data, to be displayed in context. The CMS will be built on top of the CMS Drupal 7 and provided with application programming interface (API) for direct access, via external third-party software (SW) such as Matlab, to allow effective work with large datasets.

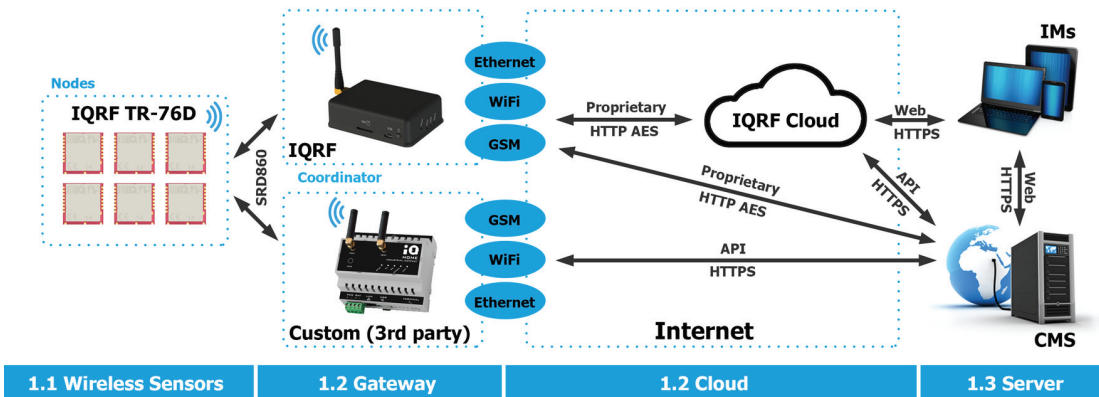


Figure 3.4: IQRF topology

Chapter 4

Realisation

Individual parts of the proposed system were analysed, designed and tested in a different order to that presented in this document and based on knowledge at the time. The individual tasks are listed below in logical sequence, signposting the sections in which they are described and explaining the decisions that led to the current technical solution.

Based on the concept described in Chapter 3 and visualised in Fig. 3.1, the feasibility test was performed and is described in Section 5.1.1. This was done primarily to resolve a discrepancy between information reported by Chraim [9] and some IMs about the required dynamic range of the inertial sensor. Next an evaluation of whether vibrations propagated ahead of an approaching train on the rail could be used to wake up the electronics in the wireless sensor, and whether data could be transmitted from close to the rails to a gateway at the desired distance. The test provided only a limited amount of data, but showed that the proposed solution is feasible and should be studied further.

The sections in Chapter 4 describe the work on the hardware design, the manufacture of the wireless sensor electronics v1.0, and the programming of the wireless sensor, the gateway and the server. At this stage a network bottleneck was discovered between the IQRF gateway and the IQRF Cloud. This issue, described in Section 5.1.2, highlighted the need for another gateway marked as v1.0. Redesigning the system to meet this requirement left insufficient time to design the wireless sensor casing, and the temporary case used eventually led to certain problems described in the following paragraph.

The system was evaluated on rails in Denmark, as described in Section 5.2. This revealed problems with the wireless sensor casing that were resolved later on by creating the proper casing. Another problem with signal reception was resolved by upgrading the gateway to v1.1 which equipped the gateway with the front-end module and external directional antenna and enclosed it in its own cabinet. The system was verified in the antenna laboratory and tested on a stacking track in Norway, as described in Section 5.3.1.

The revised system was evaluated on a track in Germany, as described in Section 5.3. The system was now fully working and provided the first useful data. This revealed an

instability problem with the time base and insufficient dynamic range of the inertial sensor, highlighting the need to revise the electronics by changing the accelerometer. During the development of the wireless sensor PCB v1.1, the ADXL372 accelerometer issues were revealed, as described in Section 5.4. These problems were studied and some were reported to the manufacturer, who investigated and recognised them. They were resolved, although some negatively impacted power use due to less efficient data handling.

The system has been deployed since February 2020 on the double crossover turnout shown at B.1a. It provides data on day-to-day basis that are released for non-commercial academic and research use. Details of the installation can be found in Paper A.3. An assessment, whether the system could meet the stringent safety integrity level (SIL) requirements for such systems today, justified that it seems possible to meet the suggested SIL requirements, which is further elaborated in Paper A.2.

4.1 Wireless Sensor

The wireless sensor’s electronics v1.0 (PCB v1.0), shown in Appendix B.1, comprise an accelerometer ADXL313, a thermometer, an SRAM memory, an RF module and a power source. Problems with time-base stability while measuring acceleration led to a revision of the electronics. The PCB v1.1 (see Appendix B.2) uses different accelerometers, ADXL343 and ADXL372, and an external crystal with 25 ppm precision, which resolve the drawbacks in PCB v1.0. These four-layer PCBs, visualised in Fig. 4.1, are enclosed in the compact casing shown in Fig. 4.2, which is optimised for use on sleepers and rail types 54E3 and UIC60. The obsolete type of casing is shown in Fig. C.1c.

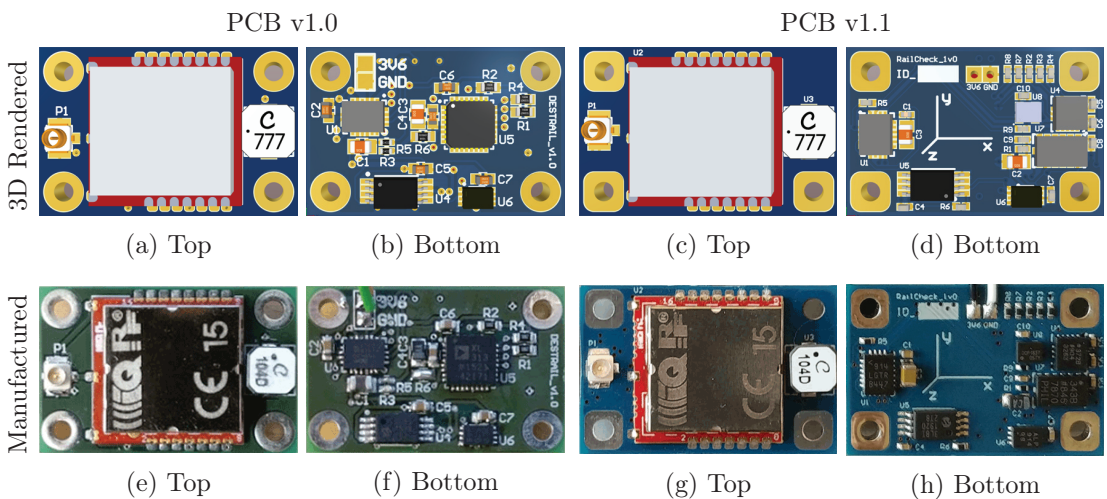


Figure 4.1: Wireless sensor PCB v1.0 and v1.1

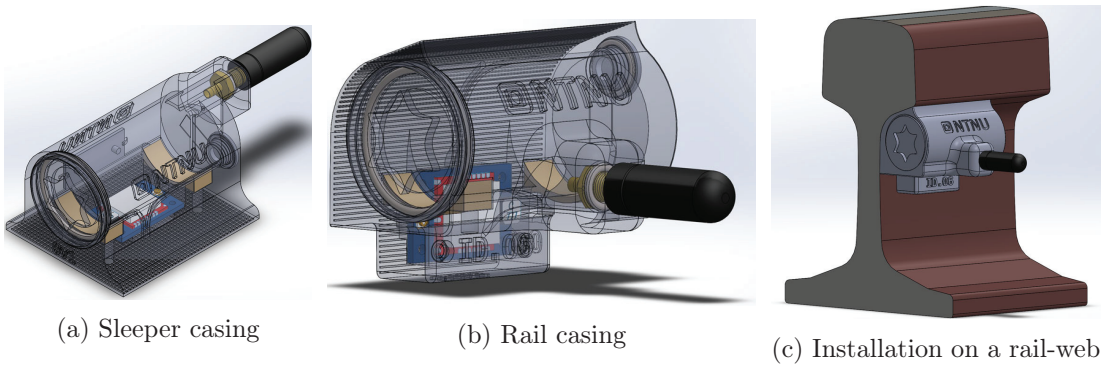


Figure 4.2: Wireless sensor casing v1.1

The user part of the firmware v1.8 without OS functions consists of 1615 lines of C code and can be split into the following categories used to group commands of the same type:

- Measure—waits for the train and begins recording when its acceleration exceeds the selected threshold. Supports [6400, 4800, 3200, 2400, 1600, 1200] Hz at $\pm 200g$ with ADXL372 and [3200, 1600] Hz at $\pm 16g$ with ADXL343.
- Fetch—transmits measurements and other parameters to the gateway. Specifically, it transmits specific or all measurement packets and gathers temperature, coulomb counter, last-sample, RSSI, activity and inactivity thresholds and counters.
- Control—contains complex functions such as for initiating data transfers with certain settings, e.g. for sending cropped or all recorded data using Fetch commands.
- Settings—change the RF mode, channel or power; set the operating mode to programming, transportation or deep sleep; reset; revert to default settings; read or write EEPROM parameters and thresholds; read the firmware version.

Of all the wireless sensor’s tasks, the data transmission uses by far the most power and takes the longest time, and as a result has the biggest impact on wireless sensor lifespan. It is essential to transfer the minimum possible amount of data with maximum possible efficiency for energy-efficient and long-lasting battery-powered operation. Many algorithms contribute to this goal: some are responsible for trimming the data so that only relevant information is transmitted while others focus on the compression and efficient handling of data within the device. One such algorithm responsible for data transfer between the inertial sensor and memory and lossless compression is shown in Fig. 4.3.

Due to the magnitude of the data they must be stored in the SRAM memory before they can be sent from the device. The HOLD function allows the memory to be initialised and paused while the accelerometer is being initialised on the SPI. This enables flipping the read-out byte from the accelerometer (MISO) to memory (MOSI) in the consecutive cycle. This is shown in the data compression function in Fig. 4.3 on the line 16.

```

1  PACKET = 0;
2  wakeupOnInterrupt(0); // Wait For MEAS Start
3  while(PACKET < PACKET_MAX)
4  {
5      getADXL372status(); // Sets param3
6      checkExitConditions(); // Break on flags
7
8      // COMPRESSION 960B*0.75=720B, FITS TO 12 PACKETS (4B HEAD + 60B PAYLOAD)
9      //-----
10     SPI_CS1 = 0; // ADXL372_CS - ACTIVE
11     sendSPIbyte(0x85); // ADXL372_CMD - READ FIFO
12     XH = sendSPIbyte(0x00); // ADXL372_READ_DATA[0]
13     XL = sendSPIbyte(0x00) & 0xF0; // ADXL372_READ_DATA[1]
14     SRAM_HOLD = 1; // SRAM_HOLD - CONTINUE
15     for(fifo=0; fifo<239; fifo++) { // ADXL_FIFO->SRAM (224*4B+4B)
16         YH = sendSPIbyte(XH); // YH XH ZH ... (E) XH
17         YL = (sendSPIbyte(YH) >> 4) & 0x0F; // YL XL ZL ... (X) XL
18         XH = sendSPIbyte(XL | YL); // ZH YH XH ... (I) YH
19         SRAM_HOLD = 0; // SRAM_HOLD - WAIT
20         XL = sendSPIbyte(0x00) & 0xF0; // ZL YL XL ... (T) YL
21         SRAM_HOLD = 1; // SRAM_HOLD - CONTINUE
22     }
23     YH = sendSPIbyte(XH); // ZH
24     YL = (sendSPIbyte(YH) >> 4) & 0x0F; // ZL
25     SPI_CS1 = 1; // ADXL372_CS - STANBY
26     sendSPIbyte(XL | YL); // SRAM_W_DATA[959] (960B)
27     SRAM_HOLD = 0; // SRAM_HOLD - WAIT
28     PACKET += 12; // 720/60B = 12 PACKETS
29 }
30 SPI_CS0 = 1; // SRAM_CS - STANBY
31 SRAM_HOLD = 1; // SRAM_HOLD - CONTINUE
32 sendSPIbyteCS1(0x7E, 0x00); // Set ADXL372 STANBY

```

Figure 4.3: Wireless sensor—compression code v1.0.3 (simplified)

Each accelerometer axis is encoded in two's complement notation of 12-bit number with a most significant bit (MSB) first. The two sample sets of the XYZ axes are read from the accelerometer as a 12 bytes and can be losslessly compressed to a 9 bytes. As demonstrated in Fig. 4.3, this is performed on the SPI bus in the following order:

- MISO [12 B]—XH, XL, YH, YL, ZH, ZL, XH, XL, YH, YL, ZH, ZL; (accelerometer)
- MOSI [09 B]—XH, YH, XL+YL, ZH, XH, ZL+XL, YH, ZH, YL+ZL; (memory)

4.2 Gateway

The original idea to use a combination of the IQRF gateway and the IQRF Cloud described in Section 3.2 turned out to be impracticable using the parameters originally anticipated, as reported in Section 5.1.2, and had to be substituted by another gateway.

Gateway v1.0, shown in Fig. 4.4, bypasses the problematic IQRF Cloud and transfers data directly to the CMS server. The gateway consists of an IQRF Universal Serial Bus (USB) gateway, an Intel Compute Stick computer and a 4G USB dongle to connect with the Internet. This configuration allows to use commercial off-the-shelf hardware and focus primarily on the software development. The C# application sends commands via the USB Communication Device Class (CDC) to the IQRF gateway, which is programmed

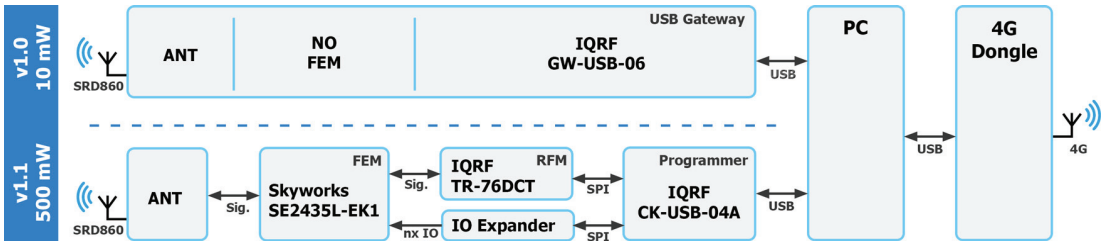


Figure 4.4: Gateway v1.0 and v1.1

to forward the commands over the air to the wireless sensors and back. The proprietary communication protocol is created to govern communications optimally.

Gateway v1.1, shown in Fig. 4.4, addresses the need revealed by the measurements performed in Denmark, as described in Section 5.2, and extends the previous gateway with the front end module (FEM). The FEM amplifies the transmitted signal, increases reception sensitivity and enables the use of two external antennas. The use of a combination of the FEM and the unidirectional Yagi antenna significantly increased the effective radiated power (ERP) to 500 mW. The gateway is equipped with a heater and is enclosed in its own cabinet to suppress negative effects of surrounding environment. The gateway software consists of 4000 lines of C# code.

4.3 Server

The website is based on the CMS Drupal. Initially, the CMS was used to retrieve data from the IQRF Cloud due to its limited capacity and unfavourable storage format corresponding to 64-byte-long packets sent from wireless sensors. CMS periodically fetched data, verified their integrity and put them together. However, due to the discovered IQRF Cloud bottleneck, described in Section 5.1.2, the IQRF Cloud was bypassed and gateway v1.0 and beyond were sending data directly to the CMS server which simplified the realisation overall. The gateway was now written in the more appropriate C# rather than procedural C, data consistency was verified right at the gateway and the data were sent to the CMS as a single HTTPS POST request in a JSON format. The CMS thus only verified the gateway’s authenticity and saved the data, reducing data traffic and increasing whole system responsiveness. Data stored on our CMS can be shown in context, displayed in graphs, loaded into third-party software, and processed efficiently.

CMS Drupal 7 (CMS v1.0) was used for measurement in Denmark and Germany. CMS Drupal 8 (CMS v1.1), now updated to Drupal 9, is being used for measurements in Norway. The CMS v1.1 has also been extended for SIRI which real-time information serves for triggering measurements of chosen trains as described in Paper A.3. The CMS module is built of—3500 PHP, 720 CSS, 340 YML, 325 JS and 260 TWIG—lines of code.

Chapter 5

Evaluation

5.1 Preliminary and Laboratory Measurements

5.1.1 Concept Feasibility Test

The preliminary feasibility test was performed during the first stage of the project to verify the concept and the performance of the components used. The main concerns were about the capacity of the electronics to wake up in time on an incoming vehicle, the magnitude of accelerometer response to an overpassing vehicle, and the ability to transmit data from a close proximity of a conductive and ground plain.

The measurement chain was assembled from the evaluation boards shown in Fig. 5.1a. The wireless sensor consisted of the accelerometer EVAL-ADXL313-Z-ND, the evaluation board DK-EVAL-04A equipped with an inbuilt battery, and the RF module TR-72DAT. Data were transmitted wirelessly to the second RF module of the same type, which was connected to the CK-USB-04A programmer and by USB cable to the computer.

The accelerometer sampling rate was set to 400 Hz and the magnitude of acceleration to ± 2 g with a sensitivity of 1 mg. The EVAL-ADXL313-Z-ND was equipped with four magnets with a thrust force of 7 kg each, which were placed on the rail-web with a total aggregated force of 28 kg, as shown in Fig. 5.1b. Measuring was triggered automatically by vibration propagated ahead of the incoming train once the level of acceleration rose above the specified threshold. Data were automatically transmitted over the structure into the C# application running on a computer which displayed them on a chart.

A light passenger train passing once in each direction was measured at a spot about hundred meters from the railway station. The incoming train was decelerating as it approached the station and passed over the sensor, as shown at the top of Fig. 5.1c. After stopping in the station, the train accelerated and passed over the sensor again on the way back, as shown at the bottom of the same figure. The measurement of the second pass was triggered manually as soon as the train moved from the station, so without the

function of sensing the oncoming train. It took the train about 7 seconds to reach the sensor and its velocity as it travelled over the sensor in each direction was about 10 kmh^{-1} .

The level of acceleration exceeded the dynamic range of the sensor which resulted in the signal being saturated visible on both characteristics of the train passings. However, if the sensor had had a maximum magnitude of $\pm 4 \text{ g}$, the signal would either be in range or would end up saturated just at the highest deflection peaks when the train's axles were above the sensor. It is expected that the transmission of vibration through the magnets was higher than it will be when the sensor is enclosed in the plastic casing that will protect the electronics from the hostile outdoor environment, as it will also introduce some damping. The accelerometer was positioned on a rail-web between the sleepers where the rail deflection is highest. The wireless sensor can be placed on the rail-web above the sleeper or, in the worst-case scenario, on the sleeper between the two rails. This should bring the values closer to those reported by Chraim [9]. If none of the above would contribute to getting into the measuring range, the inertial sensor would have to be replaced with another one from the list shown in Table 3.1.

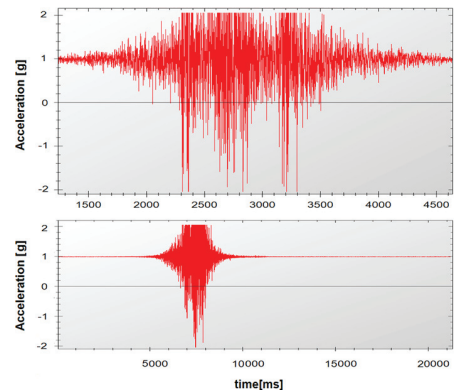
This measurement produced limited results and showed that it may be possible to measure using a $\pm 4 \text{ g}$ sensor. The wireless sensor can be woken in time by the vibrations from incoming trains cruising at low velocities, and the data can be transmitted from the sensor's position close to the rails for short distances of at least few metres. However, due to the significant uncertainty of the measurements performed, further steps should be cautiously taken and more tests should be done. This should involve the range test to verify the communication performance of gateway and wireless sensors placed on rails at various locations and different environments to find the transmission limits. Next, a multi-day test should be arranged to measure a wide range of vehicles passing wireless sensors at multiple locations, as both of these tests would clarify the system limits.



(a) Communication schema



(b) Installation of the sensor



(c) Incoming (top), outgoing (bottom)

Figure 5.1: Feasibility test on a rails in Trondheim

5.1.2 Bottleneck on IQRF Cloud

Affected devices—IQRF {GW-ETH-02A, GW-GSM-02A, GW-WIFI-01}

The original idea of using a combination of an IQRF gateway and an IQRF Cloud outlined in Section 3.2 appeared infeasible with regard to the originally-anticipated parameters. During development a communication bottleneck between the gateway and the cloud was discovered that was significantly impairing the flow of the data. As a result there was insufficient capacity to transmit the expected data volume in the given time (Fig. 5.2).

The IQRF TR-7x series, the successor to the TR-5x series, was announced at the end of 2012 and released in mid-2014 as part of the Early Adopter Program. The official release date was about a year later as we started to work on the DESTINATION RAIL project. Since the TR-7x modules offer far better parameters than their predecessor, we decided to use them. This came with certain limitations because some of their components had not been released yet. The programming was therefore realised using the substitute RF modules TR-72DAT rather than TR-76D. The same applied for the IQRF gateway, where the Global System for Mobile Communications (GSM) version was used rather than the Wi-Fi version. All of these components are identical from the programming perspective and migrating from one to another is requiring only changing the headers and loading the code into the new device, RF module or gateway. The development could thus proceed using substitute devices while planning to use others in the final installation.

During the implementation phase the communication bottleneck between the GSM gateway and the IQRF Cloud was at first attributed to technological limitations to General Packet Radio Service (GPRS) throughput, which usually reaches up to 20 to 40 kbps on upload but varies based on local coverage, the number of devices connected, and the protocols implemented in the gateway itself. This latter was later excluded as the other two types of IQRF gateways had the same issue. Investigation found that the IQRF company outsourced the IQRF Cloud to an external company which imposes an undocumented limit on the number of packets that can be transferred over a certain period of time. This led to a bizarre situation where data that could be transferred from the wireless sensors to the gateway in about 10 minutes took more than 83 minutes to be transferred to the IQRF Cloud. The situation was resolved by creating a custom gateway v1.0 that bypasses the IQRF Cloud and sends the data directly to the CMS server.

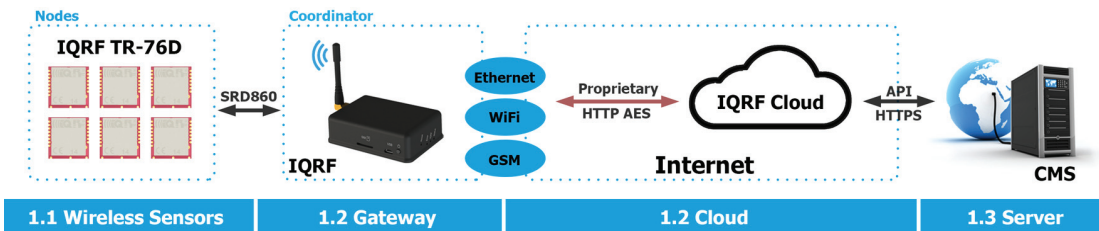


Figure 5.2: IQRF Cloud bottleneck

5.2 Measurements in Denmark

Configuration—1 location; 16·WS: PCB v1.0, WSC v1.0; 1·GW v1.0; CMS v1.0

Before the system could be deployed it had to be thoroughly tested both in the laboratory and outdoors. Time constraints did not allow us to perform tests on tracks, described in Section 5.1.1, so the system was not properly tested before its installation in Denmark.

5.2.1 Communication Gateway–CMS (Issue #1)

Communication between the gateway and the CMS worked for the first 36 hours after installation and then the gateway went offline. An occasional weak GSM signal at the measuring point was discovered. In such a case the 4G dongle attempts to reconnect only a certain number of times, and if no signal is available for an extended period it remains disconnected. This problem was fixed remotely when the system was restarted manually by railway personnel and we regained access. A batch file that tests the Internet connection every five minutes was added, and when there is no signal the device restarts and the 4G dongle automatically tries to connect to the Internet at system start up.

5.2.2 Communication Wireless Sensors–Gateway (Issue #2)

During the installation, communication between the wireless sensors and the gateway could not be established. This was due to insufficient link budget caused by the unfavourable positioning of both the wireless sensors and the gateway, and was probably also affected by other RF systems, conductive materials and reflective planes close to the gateway. A significant role here was played by the gateway's effective radiated power (ERP), which was only 10 mW of energy, which is just 2% of the energy that can be transmitted under the regulations, radiated equally in all directions perpendicular to an antenna axis and with power varying with the angle from the axis. While this should be enough to communicate over a distance of up to 1100 meters in certain conditions it was insufficient for the current constellation. Unfortunately the safety evaluation carried out earlier had stipulated that the gateway would be placed inside the existing cabinet, preventing resolution of this problem on the spot, e.g. by placing the gateway in a more favourable location. These issues were addressed by the gateway v1.1, described in Section 4.2.

5.3 Measurements in Germany

Configuration—1 location; 3·WS: PCB v1.0, WSC v1.0/v1.1; 1·GW v1.1; CMS v1.0

Based on previous unsuccessful measurements in Denmark, described in Section 5.2.2, the problematic wireless sensor casing and gateway were redesigned and tested as described in Section 5.3.1. The system was then used on rails in Germany and produced the first useful data. The description and results of this test are described in detail in Paper A.3.

5.3.1 Rail Coverage Test

The wireless sensor’s casing v1.1 is built of durable and chemically stable materials and designed to be compact. It provides improved protection against liquid ingress, and its favourable location under the rail-head makes it less prone to damage than its predecessor. The results presented in Table 5.1 show a significant improvement in the RF parameters of the new casing, with around a 6 dB increase that doubles the communication range.

The improved gateway v1.1 was enclosed in its own cabinet and fitted with a heater and an FEM, enabling the use of the external antenna and increasing both the transmitting power and the receiving sensitivity. The gateway was tested in an anechoic chamber to ensure it would not violate the 500 mW ERP limit, as shown in Section C.3.

Next, four gateway configurations and two types of wireless sensor casings were tested on a stacking track in Norway, as described in Section C.4 and Chapter IV.C of Paper A.1. Measurements in a real railway environment proved that the gateway in configuration #4 and the wireless sensor casing v1.1 greatly outperformed the configuration used during the testing in Denmark. This allowed us to schedule the next field-test in Germany.

Table 5.1: Node and coordinator RSSI for a certain distance

#	GW Configuration	ERP	Conditions		WSC	RSSI [dB]							
			1)	2)		30 m		60 m		90 m			
						N	C	N	C	N	C		
1	TR-72DCT (PWR=7) +ANT-dipole	10	2.2 m		1v0	-81	-82	NS	NS				
					1v1	-75	-75	NS	NS				
2	TR-72DCT (PWR=7) +ANT-Yagi	61			1v0	-63	-65	-78	-80				
					1v1	-59	-61	-76	-78				
3	TR-72DCT (PWR=2) +FEM+ANT-dipole	82			1v0	-72	-69	-86	-84				
					1v1	-64	-62	-82	-78				
4	TR-72DCT (PWR=2) +FEM+ANT-Yagi	500			Loc. 1	Loc. 2 covered by snow	1v0			-84	-82		
							1v1			-81	-75		
							1v0	-56	-53	-73	-71		
							1v1	-53	-51	-69	-66		
			1v0						-74	-74			
			1v1				-69	-66	-64	-62			
			1v0				-75	-75	-76	-73			
			1v1				-78	-77	-68	-66			
			1.3 m										
			1.3 m NCP						-78	-76			
									-77	-74			

ERP [mW]; **WSC** (wireless sensor’s casing); **N** (node=WS); **C** (coordinator=GW); **NS** (no signal); **Conditions—1)** Gateway antenna placed on top of n-length pole; **NCP** (near conductive plain); **2)** Situation shown on Fig. C.8d;

5.4 Measurements in Norway

Configuration—3 locations; 24·WS: PCB v1.1, WSC v1.1; 3·GW v1.1; CMS v1.1

Latest technology often pushes previous boundaries to reach new limits where new issues arise. Unless they are thoroughly tested, concealed issues get into production and can cause trouble to larger audience. This chapter reveals issues and erroneous behaviour that we reported about ADXL372 that have been officially recognised and are scheduled for resolution in forthcoming revisions. The information presented is based on datasheet, conversation with the technical support and ADXL372 developers, and ADI EngineerZone.

Problems with the inertial sensor ADXL372 were discovered before and during measurements at railway turnouts. While those identified in Sections 5.4.1 and 5.4.2 were accounted for before the system was installed on tracks, the bug described in Section 5.4.3 was discovered later and had to be addressed remotely via a firmware update.

5.4.1 ADXL372 External Clock Prescaler (Issue #1)

Accelerometer sampling is set by two registers—the output data rate (ODR) and the bandwidth (BW). The ODR controls the built-in clock, which should be set to 307.2 kHz for $\text{ODR} \leq 3200$ Hz and to 614.4 kHz for ODR above 3200 Hz. This setting configures the internal circuits to suit the given sampling rate; specifically, higher oscillator frequency entitles circuits to substantially increased power use. In addition, the ODR setting changes the analog-to-digital converter (ADC) sampling rate, which acts as a clock frequency divider (of 2^n , $n \in \{1, 2, 3, 4\}$), allowing the creation of a discrete number of ODR options. The BW, on the other hand, changes the architecture of the front-end anti-aliasing filter without affecting the ODR to satisfy the Nyquist criteria by setting the BW to at most half of the ODR, which must be set and ensured by user. When desired, an external clock source can be used to improve the clock frequency accuracy and to achieve any desired ODR outside the discrete number of options as a result of the ODR and BW scaling ratiometrically with the clock signal applied.

Due to the construction of the accelerometer the ADC prescaler is not available when an external clock source above 307.2 kHz is used. This is not explained well on the manufacturer's datasheet and there is no comprehensive description or diagram available. Upon request, ADI provided us with additional information so that we could draw a more detailed diagram, shown in Fig. 5.3. The dashed rectangle indicates the known diagram.

The wireless sensor in PCB v1.1 utilised the external clock feature and was fitted with an oscillator providing 460.8 and 614.4 kHz, which limited the ODR configuration to above 3200 Hz. This prevented internal scaling, so we could not achieve ODRs other than 4800 Hz and 6400 Hz from the following expected combinations [6400, 4800, 3200, 2400, 1600, 1200, 800, 600, 400, 300] Hz. To resolve this, the expected combinations had to be achieved using a firmware function that stored only the n th set of samples read from the accelerometer. This had a negative impact on the duration for which the sensor

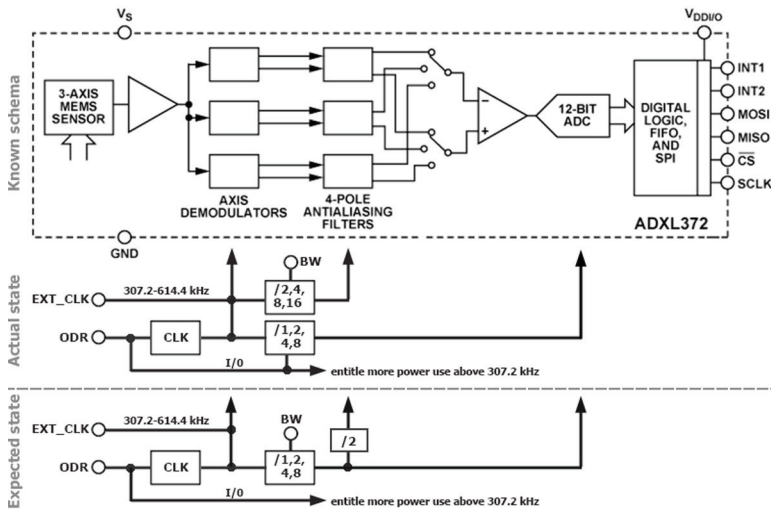


Figure 5.3: ADXL372 schema

could stay asleep, as the FIFO buffer filled much faster and had to be serviced more often than if the sensor were designed to support such scaling in all settings.

A better solution may be for the ODR to control the oscillator frequency and the BW to control the prescaler of ADC sampling with a fixed BW divider by two for anti-aliasing filters. This would address all possible combinations as shown in Fig. 5.3 in 'Expected state'. In such case, the ODR should be renamed to CLK_SEL and BW to ODR.

5.4.2 ADXL372 FFT ODR/5 Noise (Issue #2)

In 2018 the ADI EngineerZone user naohisa revealed the fast Fourier transform (FFT) noise at ODR/5 that is caused by the sensor material [12]. While the datasheet's RMS noise accounts for all noise sources, the ODR/5 is not specifically mentioned. This noise appears on FFT as significant peaks which must be accounted for during data analysis.

5.4.3 ADXL372 Data Misalignment in FIFO Stream Mode (Bug #1)

The data misalignment issue in FIFO stream mode was investigated by the manufacturer as a timing-related problem with the internal FIFO architecture at our request, and soon afterwards it was officially declared a post-silicon bug. This issue seems likely to have been present since the part was released in 2017, as several users had already reported it; however the ADI had not been successful in reproducing this erroneous behaviour based on their reports. The official recommended way of getting around this is to use the FIFO in the bypassed mode. Doing such negatively impact power use and noise performance.

The core of this problem is that the accelerometer in the FIFO stream mode disposes of the FIFO buffer content before it has been fully read. The FIFO_ENTRIES register sometimes reports 0 valid samples in the FIFO buffer regardless of the initial number of samples and of bytes being read. For example when FIFO is filled with 483 samples of which it has read 480, it should report at that least 3 valid samples remain, as indeed it does when the accelerometer is working. However, sometimes the FIFO_ENTRIES register reports 0 valid samples after a FIFO read; this reading usually stays hidden as the register is typically read prior to the FIFO read. The empty FIFO buffer then breaches the rule that there must be at least one sample set (series) left in the buffer after every consecutive read. This issue is therefore often accompanied by data misalignment, as the accelerometer cannot identify the series start indicator bit in the FIFO buffer.

This issue can be identified by reading the FIFO_ENTRIES register both before and after reading the FIFO. This is to verify that FIFO_ENTRIES after reading FIFO holds the same or a greater number of bytes than before the FIFO reading was initiated and subtracted from the number of bytes read from the FIFO. If this is not the case some bytes have got lost, which may lead to data being misaligned. If the data are misaligned this issue can also be identified by monitoring the series start indicator flag, which moves from the first axis to any random other one in the data. This can be visually observed in charts as axes periodically switching places, as shown in Fig. 5.4. In our case, this incorrect behaviour was occurring approximately every third measurement of 21k sample sets at 6400 Hz, regardless of the number of axes captured, and its incidence was decreasing with ODR. The FIFO_ENTRIES in these cases suddenly reset (to zero) while the FIFO_RDY still correctly indicates at least one valid sample available in the FIFO. Completely bypassing the FIFO avoids the issue, producing somewhat more noise than the sensor in the FIFO stream mode. The voltage stability on accelerometer Vdd and Vaa power lines was comparable throughout the measurement in both of these modes.

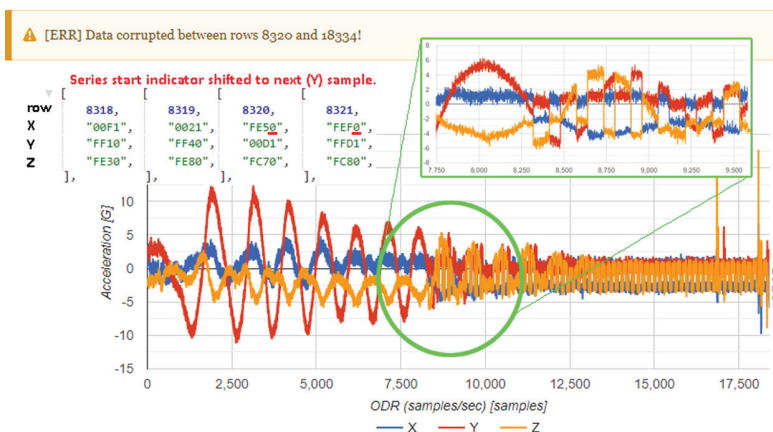


Figure 5.4: ADXL372 data misalignment bug

Chapter 6

Conclusion

This thesis investigates the potential of consumer-grade micro-electromechanical systems (MEMS) inertial sensors for the remote monitoring of vehicle-track interaction on railway turnouts. Railway turnouts are the only subsystem of the railway superstructure that consists of moving parts, and are therefore subject to stronger dynamic forces that make them more susceptible to wear, defects and failure. While nominal track can be automatically inspected by equipped measurement trains (EMT), these methods are not suited to the inspection of railway turnouts and must be conducted manually, making turnout maintenance both time-consuming and cost-ineffective.

The solution to this issue must be economically advantageous compared to the status quo, and it must be as or more reliable than current methods. The indisputable advantage of track-side systems is its more frequent remote monitoring on demand, improved supervision of degradation processes and optimal scheduling of maintenance intervals as required. This can eventually be made possible by systems such as proposed RailCheck system, which uses an inexpensive sensors that are consisting of a MEMS accelerometer, a battery and a radio-frequency module. These sensors records vehicle-track interactions and transfers the data to the server for analysis, processing and storage. Pilot testing has shown that when the bandwidth and noise performance are acceptable, affordable MEMS accelerometers can provide sufficient data for a fraction of the cost of industrial sensors. Powered by batteries, they can also last for years and in time, promise effective monitoring of railway assets that require more frequent inspection.

A number of initial steps required to apply IEC 61508, EN 50126 and EN 50159 have been studied and demonstrated in a published Paper [A.2](#). The context of use, potential hazards and safety integrity level (SIL) requirements that may be imposed on this system are clarified. An initial dysfunctional analysis was carried out to justify the idea that it seems possible to meet the suggested SIL requirements with respect to systematic and random hardware failures. Further work should include a more detailed analysis of failure rate estimates and other measures imposed by the SIL requirements,

for instance regarding the avoidance and control of software faults in the development of the application program. The paper has also reviewed ways of considering security along with safety design. The wireless technology and devices that may be accessed by anyone entering the tracks means that no system such as this can be safe if it is also not secure.

The RailCheck system was designed, built and verified on tracks in Denmark, Germany and Norway. One of our assessments revealed insufficient dynamic range of the sensor and poor time-base stability, rendering it unsuitable for efficient data processing. These issues were resolved by using a different inertial sensor, and the revised system was deployed as a permanent test bed on the busiest section of Norway's railway network. Data from a double crossover turnout were collected for a over a year and released for non-commercial academic and research use. The availability of a real non-ideal datasets as a basis for simulations, algorithm development and method verification lays the foundation for the creation of reliable algorithms that may be directly applied to an affordable real-time measurement systems. This will eventually allow automatic analysis of the state of track and enable the desirable smooth transition from preventive to predictive maintenance. The remaining problem is the lack of sufficient digitisation and system interconnection to enable the provision of supplementary information about passing vehicles. This would be useful for the development of reliable algorithms and their proper functioning. Some of this information is expected to become available with the implementation of the European Rail Traffic Management System (ERTMS) and following revisions of the Service Interface for Real-time Information (SIRI).

To conclude, the results and experiences of this project indicate that systems such this has strong potential and will play a crucial role in future transportation systems. Inertial MEMS sensors and electronics in general will undoubtedly evolve to provide better data overall at lower cost and power consumption. ERTMS will moreover minimise the cost of data transmission and make a system such this one economically interesting. Therefore it is important to develop robust algorithms and methods for processing the data so that infrastructure managers can take advantage of the potential of these systems.

References

- [1] Elias Kassa, Jan Sramota, and Amir Kaynia. Deliverable 1.3 Report on monitoring Switches and Crossings. Technical report, DESTination RAIL, 2017.
- [2] Jan Sramota and Amund Skavhaug. RailCheck: A WSN-Based System for Condition Monitoring of Railway Infrastructure. In *2018 21st Euromicro Conference on Digital System Design (DSD)*, pages 347–351. IEEE, 2018. doi: 10.1109/DSD.2018.00067.
- [3] Jan Sramota, Mary Ann Lundteigen, Stig Petersen, and Amund Skavhaug. RailCheck: Functional Safety for Wireless Condition Monitoring of Railway Turnouts and Level Crossings. In *2019 IEEE Intelligent Transportation Systems Conference (ITSC)*, pages 3188–3193. IEEE, 2019. doi: 10.1109/ITSC.2019.8917093.
- [4] Jan Sramota and Amund Skavhaug. RailCheck Dataset of Vehicle-Track Interaction Measured on Railway Turnouts. In *TBS*, page TBS. TBS, 2021. doi: TBS.
- [5] Coenraad Esveld and Coenraad Esveld. *Modern Railway Track, Second Edition*, volume 385. MRT-productions Zaltbommel, 2001. ISBN 90-800324-3-3.
- [6] Malcolm Kerr. TMC226: Rail Defects Handbook. Technical report, RailCorp, 2012.
- [7] Malcolm Kerr. TMC227: Surface Defects in Rails. Technical report, RailCorp, 2013.
- [8] Mykola Sysyn, Olga Nabochenko, Vitalii Kovalchuk, Dimitri Gruen, and Andriy Pentsak. Improvement of Inspection System for Common Crossings by Track Side Monitoring and Prognostics. *Structural Monitoring and Maintenance*, 6(3), 2019.
- [9] Fabien Chraim and Sravan Puttagunta. Monitoring Track Health Using Rail Vibration Sensors. www.academia.edu/7833123/Monitoring_Track_Health_Using_Rail_Vibration_Sensors, 2014. Accessed: 2021-01-01.
- [10] IQRF. TR-76D: RF Transceiver Module Series (Data Sheet). <https://www.iqrf.org/product-detail/tr-76d>, 2015. Accessed: 2021-01-01.
- [11] Xiaopei Cai. Detection of Acceleration Sensitive Areas of A Rail and Railway Switch Using Dynamic Analysis. N/A, 2015. Accessed: 2021-01-01.

- [12] naohisa (ADI EngineerZone). ADXL372 peak noise for FFT. <https://ez.analog.com/mems/f/q-a/91005/adxl372-peak-noise-for-fft>, 2018. Accessed: 2021-01.

Appendices

Appendix A

Publications

Paper A.1

RailCheck: A WSN-Based System for Condition Monitoring of Railway Infrastructure

RailCheck: A WSN-Based System for Condition Monitoring of Railway Infrastructure

Jan Sramota, Amund Skavhaug
Department of Mechanical and Industrial Engineering
Norwegian University of Science and Technology
Trondheim, Norway
Email: {jan.sramota, amund.skavhaug}@ntnu.no

Abstract—Contemporary tools used to monitor railway points and crossings are ineffective. Routine inspections of these critical parts are still being performed manually by specially-trained inspectors. This creates higher expenditure and makes infrastructure difficult to maintain. With the expected further expansion of the railway network, this exerts increased pressure on infrastructure managers to ensure safe and predictable traffic. Hence there is a need for inexpensive and reliable condition-based maintenance systems. This paper describes an autonomous, near-real-time system built to this effect. It is based on acceleration measurements of train-track interaction, when the train is present. Using a wireless sensor network (WSN), data are aggregated over the Internet of Things (IoT) low-power wide-area network (LPWAN) structure into the Internet, where the big-data post-processing is performed. The performance and suitability of this system were evaluated on tracks in real traffic conditions and were found to be potentially beneficial for this sector. The system was built over a three-year period as part of the DESTinationRAIL H2020 EU-project.

Keywords—IoT, condition monitoring, condition-based maintenance, LPWAN, WSN, LTE-R, IQR, railway

I. INTRODUCTION

Worldwide railway networks have more than 1.15 million km of rail tracks [1], with further expansion planned. This inevitably requires methods and tools for the effective health monitoring of these large transportation networks.

Rail tracks without points and crossings are today regularly inspected by equipped maintenance trains that use camera or laser-based systems to automatically evaluate their condition. These tools, especially the laser-based solutions, can operate at very high speeds of up to 450 kmh^{-1} , and are an effective solution to gathering a large number of very precise datasets that can be further processed with relative ease. A support decision system can autonomously conclude where to increase inspection intervals, set a schedule for maintenance, and decide which rails need to be fully replaced, having reached the end of their life. Before these methods existed, railway inspectors were dependent on many local measurements which were performed manually and one at a time. Decisions to replace tracks were frequently made at inappropriate moments, sometimes long before it was necessary or much too late in the life-cycle of the track. Contemporary tools for monitoring the geometric quality of tracks allows more frequent inspection, predictive maintenance control, and use of the existing infrastructure with high efficiency throughout the whole life-cycle.

The situation at railway points and crossings (P&C), on the other hand, is significantly different. Existing tools for monitoring degradation processes on P&C are not fully applicable on these parts. Furthermore, track-stiffness-monitoring vehicles cannot be used for these sections either. While spending on the maintenance and renewal of rail track without P&C is constantly optimized, expenditure on P&C has remained rather rudimentary over the decades. Degradation processes are still solely inspected manually, which, in combination with the large number of these parts, leads to high spending and ineffective maintenance. In some countries [2] about 25% of all maintenance costs are still being allocated to these critical parts. To resolve this disproportion new systems must be developed. One such system, RailCheck, has recently been introduced by Norwegian University of Science and Technology as part of the DESTinationRAIL [3] project.

II. STATE OF THE ART

Systems addressing this problematic are usually train or infrastructure-based or a hybrid of both.

Train-based solutions use sensors mounted on the train's suspension to evaluate responses from the tracks. The advantage of this method is its ability to filter out, to a certain extent, the response of its own, suspension. The disadvantages are the large amount of captured data and difficult recognition of the current position over the specific P&C. The train-based solution may be the most interesting future method, since modern trains are often already equipped from stock by very precise vibration sensors for the train's own self-diagnosis. If these data become accessible they might offer a very cost-effective and elegant way of gathering large numbers of representative datasets.

Infrastructure-based solutions [4] are currently the most feasible approach to railway condition-based maintenance. Stationary sensors mounted directly on the rails detect vibrations from passing trains at specific preselected P&C, and data are transmitted through existing GSM/WLAN infrastructure. The main disadvantage is the higher cost due to the large numbers of sensors in the network.

The hybrid solution [5] is usually an attempt to use stationary sensors mounted on the rails and a gateway located on the train. The main difficulty is the transmission of data between the fast-moving train and the sensors.



Fig. 1. Proposed condition monitoring system

III. PROPOSED CONCEPT

As the RailCheck system was built as a deliverable of the DESTINATIONRAIL EU project [3], many of its operational parameters were already defined. Thus this concept could become the base solution for other, similarly defined systems.

Due to the large number of P&C in the railway infrastructure there is a large demand for systems that are both reliable and inexpensive. These two parameters can be broken down into detailed sub-terms, each with its own implications. The system must be secure, safe, maintenance-free and easy to deploy. It is assumed that solutions will be wireless and battery-powered, and will allow a high level of integration with existing and future railway structures. There are also performance-related requirements: the system should operate continuously in real time, and be capable of processing and storing data to enable the next steps in autonomous monitoring.

The proposed sensory system shown in Fig. 1 is based on common IoT LPWAN conventions. It provides autonomous near-real-time data acquisition, data aggregation and processing, and forwards information on the state of the infrastructure to stakeholders. Passing trains, both ordinary and monitoring, have access to these data. WSN and its support decision part facilitates responses to unexpected critical situations and the performance of optimal condition-based maintenance.

The basic idea for the data processing is based on long-term monitoring of the same unique trains over time based on prior knowledge of their configuration and cruising speed. E.g., by monitoring just one specific train every day, gradual changes in train-track interaction can be observed. The collected data would contain information about the train's suspension, the state of the track, and unpredictable events such as the impacts of a train's wheel flange hitting the rail head. This will make it possible to distinguish between the sources of such events and suggest actions to optimize spending.

A. Wireless Sensors

Wireless sensors in LPWAN are often battery-powered and are designed to operate for up to more than a decade. To achieve this, the sensors must sleep most of the time and only wake to perform their monitoring and communication tasks. The average current in sleep mode is typically at nA scale and μA during monitoring, sometimes rising to units of mA for radio frequency (RF) transmissions. Efficient power management and low costs are the most important requirements for the hardware.

1) *MEMS Accelerometer*: Most of the current measurements on the rails are performed by industrial-grade sensors that capture data at high sampling frequencies of 10-25 kHz, and measure acceleration up to ± 500 g. For our application this is less than ideal, due to the high initial costs, high power consumption, large size, lack of connectivity and difficult power-efficient transmission of generated data. In addition, these instruments are usually general-purpose, which can result in unneeded data and subsequently in unnecessary processing and communication. The primary objective therefore was inexpensive sensors with a limited range and data sampling-rate that could provide usable data, containing all the necessary information. Based on Fabien's [5] findings, a four-dollar MEMS accelerometer, ADXL313 [6], commonly used in consumer electronics, was selected. It has a limited dynamic range of ± 4 g with a maximum sampling rate of 3.2 kHz and uses barely $170 \mu\text{A}$ of energy. The sensor consumes $55 \mu\text{A}$ during sleep and has a wake-up feature. The indisputable advantages of using this consumer-grade sensor are the desirable price and the low power consumption.

2) *Battery & Power Supply*: Applications designed to last for decades require new approaches to power management. Commonly used batteries self-discharge too fast, therefore a 7.7 Ah cells based on Lithium-Thionyl chloride (Li-SOCl₂) chemistry were necessary. These are designed specifically for long-term, 3-15 year application, and featuring a few μA base current. They are intended for periodic pulses, typically in the 5-150 mA range. Similar considerations apply to the voltage regulator, which has to have very high efficiency and a low quiescent current. Therefore LTC3335 [7], a nano-power buck-boost DC/DC with an integrated coulomb counter, was chosen. This regulator can monitor how much energy has already flowed through its circuits.

3) *Wireless Communication*: The sensors' wireless transmission is among the most energy-demanding tasks, and is therefore typically reduced to the minimum necessary. The market offers various solutions with transceivers with differing transmission speeds and ranges, frequencies used, protocol overheads, costs, and predominantly power consumption. The ISM band SRD860 with peer-to-peer communication was chosen based on the Spirit1 circuit [8]. This uses GFSK modulation and AES-128 encryption, and with an actual transmission rate of 19.8 kbps it can deliver data up to a distance of 500 m with 21.5 mA current consumption. This

device can stay responsive in receiver mode with just 16.3 μ A of energy overheads. To reduce the power consumption and overall costs, the wireless module's microcontroller was also used for all of the sensor's processing and control tasks.

4) *Sensor Casing & Location*: The wireless sensor's integral casing contains all the crucial parts needed to power the circuits, record acceleration data from the approaching trains, and to store and eventually pre-process these data before transmitting them to the LPWAN. The compact casing simplifies handling, allowing rapid and easy deployment.

The position of the sensors on the rails was selected based on current legislation (Norwegian, also applies in the EU), RF propagation properties tested at Chapter IV-C, and previous research examining how acceleration varies with different measuring locations [9]. Six preselected positions on a rail head, rail web and rail foot between and above the sleeper, and two locations on top of the sleeper, in the middle and at one end, were evaluated. It was decided to use the upper part of the rail web directly below the rail head between the sleepers for the rail measurements (Fig. 2c), and the middle of the sleeper for sleeper measurements. The rail casing (Fig. 2b) is currently compatible with two types of rail profile: 54E3 and UIC60. Universal casing (Fig. 2a) supports horizontal or vertical mounting, e.g. on the railway sleeper.

The sensor casing was designed to address the requirements of chemical stability, durability, casing stiffness, waterproofness and signal propagation. Emphasis was placed on limiting the vibrations and resonant frequencies that would otherwise lessen the value of the measurements from the rails. ABS plastic, used in early prototypes, was found to be unusable due to its sensitivity to UV light and lack of chemical stability. Polyamide PA2200 was used as a replacement.

B. Gateway

The gateway is the main element in the communication chain, with unidirectional control over the sensors. A coordinator-node half-duplex communication is realized with a line of sight of up to 500 m. The gateway is placed close to the sensors, usually along the rails on the catenary mast (Fig. 2d), and creates a local cell with the sensors that it covers. The gateway accepts commands from parenting structures; however, it decides the order of their execution based on its current state. This creates a robust, distributed and highly scalable system. The gateway is responsible for the wireless sensor actions, for data consistency, and for forwarding the data and other (meta) information to the Internet-based storage.

1) *Electronics*: The original idea, to use third-party products, a combination of IQRF Gateway [10] and IQRF Cloud [11], was found to be incompatible with the qualitative requirements of the DESTINATIONRAIL project [3], primarily due to the undocumented bottleneck between these two parts. Therefore a dedicated gateway of our own design was built to address the project's requirements. The effective radiated power (ERP) was increased by a front-end module (FEM) [12] and a SRD868 10 dBi Yagi antenna from 12.5 mW to 500 mW. The receiver's sensitivity was increased by the same measures.

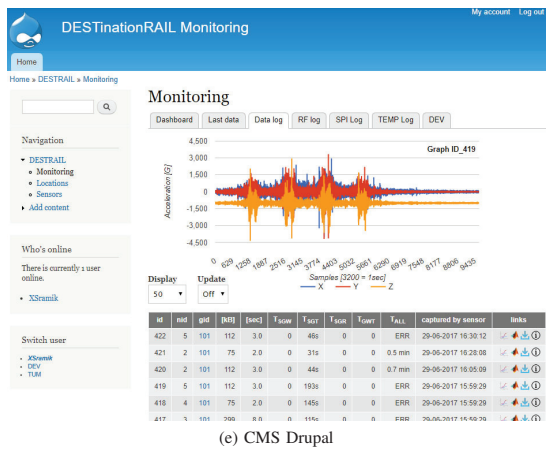
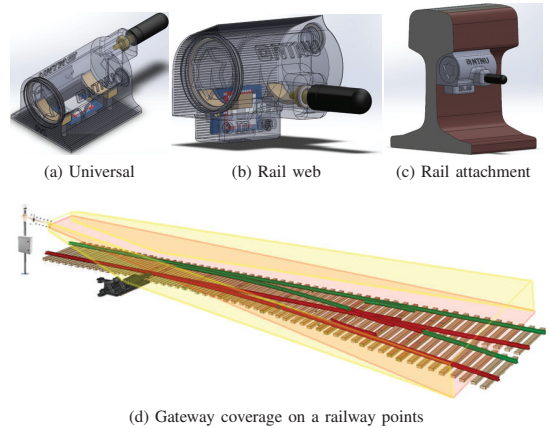


Fig. 2. Wireless Sensor Casing (a,b,c); Gateway (d); Web server (e)

Support for communication over both WiFi 802.11ac and LTE networks (LTE-R in future revisions) was added to the design.

2) *Gateway Casing & Location*: The gateway electronics were enclosed in a cabinet of 300x200x150 mm, with provisions for mounting it on a pole or catenary mast. The Yagi antenna was directed along the rails towards the sensors.

C. Web server

The web-based content management system, Drupal [13] (Fig. 2e), serves several purposes. Mainly it is used as an aggregation point for all of the sensor's data, which are stored, analysed and displayed in context here. Authorized users are granted access through the HTTPS protocol and can use various services, such as export to MATLAB, for subsequent work. Data can also be automatically propagated to key stakeholders such as railway inspectors, passing or monitoring trains.

IV. EVALUATION

This section describes the evaluation primarily of the hardware. A detailed evaluation of the data from the experiments is being prepared for publication in a railway-specific journal.

A. Feasibility test

A feasibility test of the preliminary concept was performed during the first stage of the project to assess the performance of the crucial components and their key features and parameters. The main concerns were the accelerometer's capability to wake up the electronics on an approaching train¹, its response on an overpassing trains¹ and the ability to transmit the data acquired over radio frequencies, as elaborated in Chapter IV-C.

A measurement chain was assembled from several evaluation boards, as shown in Fig. 3a. The wireless sensor consisted of accelerometer EVAL-ADXL313-Z-ND [6], a battery-powered board DK-EVAL-04A [14], and an RF module TR-72DAT [15]. The gateway consisted of a second RF module, a programmer CK-USB-04A [16], and a computer. Measuring was triggered automatically by the oncoming train once the acceleration superseded the threshold specified. The data were automatically transmitted over the whole structure into the C# application running on the computer. The application recorded RAW data in the file and displayed them as a chart.

For practical reasons in this specific test, the accelerometer sampling frequency was set to 400 Hz with a gravity range of ± 2 g, and vertical axis measuring deflection only was recorded. According to similar measurements taken by Fabien [5], the selected magnitude of acceleration should be appropriate. The accelerometer was then attached to the rail web using four magnets with a total aggregated force of 28 kg, as shown in Fig. 3b.

Two passenger trains passing in each directions were recorded at a spot about 100 m from the railway station. The incoming train slowed down approaching the station and passed over the sensor as shown in Fig. 3c. Afterwards the train accelerated away from the station and in about 5 seconds passed over the sensor in the opposite direction. This time the measurement was triggered manually once the train moved from the station, as shown in Fig. 3d. The speed of the train over the sensor was in both cases approximately 10 kmh^{-1} .

Both of the measurements shown in Fig. 3c and Fig. 3d went into a saturation when the train's acceleration exceeded the selected magnitude. From this and further results obtained later, the following assumptions were made: firstly, as expected, a sampling frequency of 400 Hz is not suitable for such a measurement, since many of the useful data are filtered out. The 3200 Hz used in following tests appeared to be an adequate minimum. Secondly, accelerations measured by consumer-grade sensors, which have a lower sampling rate than commonly-used industrial sensors, are much lower than what these sensors usually measure. Thirdly, wake-up on the approaching train is possible due to the sensor's response time

¹Data are being prepared for publication in a railway-specific journal.

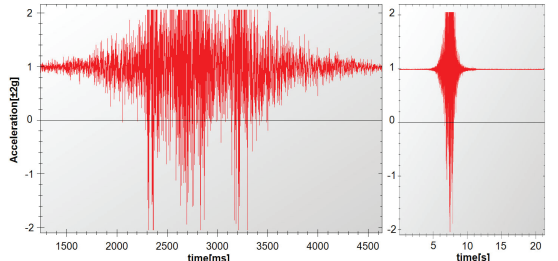


Fig. 3. Feasibility test

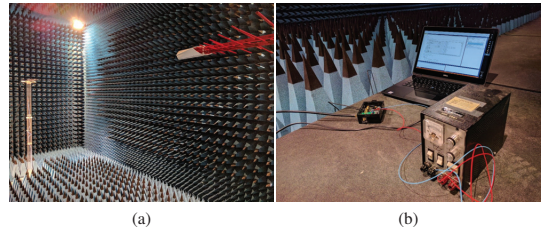


Fig. 4. Anechoic chamber test

of up to 1.4 ms at 3200 Hz, when the acceleration rises over the selected threshold¹. The accelerations of about $\pm 100 \text{ mg}$ 1 sec and $\pm 200 \text{ mg}$ 400 ms were sensed before the train passed over the sensor at 160 kmh^{-1} during another test.

B. Validation of Gateway ERP

Before the system could be used outside the controlled environment it had to be verified against current legislation, which is governed by ETSI regulation for SRD860 devices operating in the ISM band: ECC Recommendation 70-03 [17]. This was done in an anechoic chamber, as shown in Fig. 4, where all the parts involved in signal propagation were validated as a whole against the reference antenna. Due to known RF attenuation in used coaxial cables and air attenuation of known distance, the correct parameters were calculated and set to the RF circuits. This allowed us set the output constants properly and verify that not more than 500 mW ERP will be radiated from the

gateway, to prevent RF interference between various systems, which could be dangerous, especially on the railway.

C. Verification of coverage between sensors and gateway

The practical evaluation was performed on a stacking track, as shown in Fig. 5a, in cooperation with Bane NOR. Sensors were deployed at 30, 60 and 90 m from the gateway, which was attached to a pole of height 1.3 and 2.2 m. The 30 m point was marked with an orange-and-white traffic cone, an orange-and-yellow traffic cone next to the concrete sleepers marked the 60 m point, and for the 90 m point, the gateway was relocated 30 m backwards along the track.

The results presented in this chapter are indicative only and are not statistically significant, nor are they necessarily representative of other sites or weather conditions. The tests were performed within a limited time span, with the main purpose to evaluate the reliability of the communication between the sensors and the gateway. For general applicability and statistical validity we would need long-term installations in several places, something that clearly must be done before the commercialization of this concept.

The main concerns regarding signal propagation due to the deployment of sensors directly to the rail body appeared to be valid. Signal propagation from the sensor was highly affected based on the antenna's location against the rail. Even small changes in location from the first prototype to the second were reflected by an increase of 6 dB at some of the measurements. This was achieved by moving the antenna from the rail web about 2 cm vertically and 2 cm horizontally from the rail body. Another positive finding was that the 10 cm column of snow shown covering the sensors in Fig. 5d, did not reduce signal quality. This was probably strongly affected by the favourable weather conditions with several cold days ahead of the test, the snow was therefore very dry. Trains passing during active transmission did not seem to interfere with communication.

Due to the limited length of the stacking track, the communication between sensors and gateway was tested only to a distance of 90 m. The gateway was located on a pole 2.2 m above the terrain and the sensors were covered by a 10 cm column of dry snow. The test was performed in favourable weather conditions: a sunny day with -12°C . Reliable communication was achieved with a signal strength of over -62 dBm. With receiver sensitivity of -115 dBm and the presumption that each 6 dB gain doubles the effective range, reliable coverage of 250 to 500 m can be expected.

V. CONCLUSION

Results from a designed, implemented and deployed WSN-based system, RailCheck, revealed that even inexpensive consumer-grade accelerometers may be suitable as a basis for obtaining necessary data for the purpose of condition monitoring and subsequent condition-based maintenance of railway tracks, points and crossings. Affordable wireless sensors costing about €20 per unit might accelerate the use of these sensors and allow their deployment on a large scale. The results and experiences of this project indicate that systems



(a) Antenna coverage test



(b) Gateway location

(c) Sensor placement

(d) Sensors under snow

Fig. 5. Coverage test

such as the one presented here will have a crucial role in future transportation systems.

REFERENCES

- [1] Central Intelligence Agency World Factbook. <https://www.cia.gov/library/publications/the-world-factbook/fields/2121.html>. Accessed: 2018-04-01.
- [2] W.-J. Zwanenburg. *Modelling Degradation Processes of Switches & Crossings for Maintenance & Renewal Planning on the Swiss Railway Network*. PhD thesis, EPFL, 2009.
- [3] DESTINATIONRAIL. <http://www.destinationrail.eu>. Accessed: 2018-04-01.
- [4] V. J. Hodge, S. O'Keefe, M. Weeks, and A. Moulds. Wireless sensor networks for condition monitoring in the railway industry: A survey. *IEEE Transactions on Intelligent Transportation Systems*, 16:1088–1106, 2015.
- [5] F. Chraim and S. Puttagunta. Monitoring track health using rail vibration sensors. www.academia.edu/7833123/Monitoring_Track_Health_Using_Rail_Vibration_Sensors. Accessed: 2018-04-01.
- [6] Analog ADXL313. www.analog.com/en/products/sensors-mems/accelerometers/adxl313.html. Accessed: 2018-04-01.
- [7] Analog LTC3335. www.analog.com/en/products/power-management/battery-management/coulomb-counter/ltc3335.html. Accessed: 2018-04-01.
- [8] ST Microelectronics SPIRIT1. www.st.com/en/wireless-connectivity/spirit1.html. Accessed: 2018-04-01.
- [9] X.P. Cai and E. Kassa. Detection of acceleration sensitive areas of rail using a dynamic analysis. *Proceedings of the Third International Conference on Railway Technology: Research, Development and Maintenance*, 2016.
- [10] IQRF GW-WIFI-01. www.iqrf.org/products/gateways/gw-wifi-01. Accessed: 2018-04-01.
- [11] IQRF Cloud. www.iqrf.org/technology/iqrf-cloud. Accessed: 2018-04-01.
- [12] Skyworks SE2435L. www.skyworksinc.com/Product/938/SE2435L. Accessed: 2018-04-01.
- [13] Drupal - Open Source CMS. www.drupal.org/. Accessed: 2018-04-01.
- [14] IQRF DK-EVAL-04A. www.iqrf.org/products/development-tools/development-kits/dk-eval-04a. Accessed: 2018-04-01.
- [15] IQRF TR-72D. www.iqrf.org/products/transceivers/tr-72d. Accessed: 2018-04-01.
- [16] IQRF CK-USB-04A. www.iqrf.org/products/development-tools/development-kits/ck-usb-04a. Accessed: 2018-04-01.
- [17] ERC Recommendation 70-03. www.erodocdb.dk/Docs/doc98/official/pdf/REC7003E.PDF. Accessed: 2018-04-01.

Paper A.2

**RailCheck: Functional Safety for Wireless
Condition Monitoring of Railway Turnouts
and Level Crossings**

RailCheck: Functional Safety for Wireless Condition Monitoring of Railway Turnouts and Level Crossings

Jan Sramota, Mary Ann Lundteigen, Stig Petersen, Amund Skavhaug

Department of Mechanical and Industrial Engineering

Norwegian University of Science and Technology

Trondheim, Norway

Email: {jan.sramota, mary.a.lundteigen, stig.petersen, amund.skavhaug}@ntnu.no

Abstract—Increasing demands for more cost-effective, reliable and safer railway infrastructure unavoidably bring up the need for transitioning from current preventive maintenance strategies to more efficient, predictive, condition-based maintenance models. Such a change requires large installations of sensors that continuously monitor key infrastructure and aggregate captured data for post-processing in the cloud. Due to the amount of assets to be supervised, novel approaches must be studied in order to find a viable solution that is deployable on this scale. Continuous surveillance is then a desired goal, as it is closely associated with big-data analytics and allows to predict upcoming issues and react to unexpected events. Infrastructure managers will gain much better overview as a result of large amount of highly representative data set-in-context; moreover, they will benefit from having supportive algorithms simplifying their determinations. This paper describes the safety-related measures performed on one such system; eventually intended to replace the routine inspections currently being carried out on railway points and level crossings.

I. INTRODUCTION

Increasing demands for better transportation systems in the 21st century resulted in a trend called *smart transportation* and facilitated the emergence of *intelligent transportation systems*. These systems aim to minimise traffic problems, enrich stakeholders with prior knowledge, reduce travel time and cost as well as enhance passengers' comfort and their safety. Indeed, between today and 2050, major changes are expected due to previous increased activity in this area [1].

Speaking at the operational level, the European Rail Traffic Management System (ERTMS) [2], which provides a common framework for all railway traffic in Europe, was adopted and is now being implemented. The ERTMS comprises the European Train Control System (ETCS), railway adaptation of the Global System for Mobile Communications (GSM-R) [3][4] and the European Traffic Management Layer. Interestingly, work that started on ETCS in the early 90s revealed number of challenges that either affected or resulted in several safety-related and technological standards, including e.g. IEC 61508 [5], EN 50159, GSM-R and the forthcoming LTE-R [6]. It remains an open question whether or not LTE-R will be launched as a successor to GSM-R (as happened in South Korea), or if the next generation '5G-R' will be used instead. However, it is expected that ERTMS at level 3, having the potential to increase the capacity up to 40% on the current infrastructure [7], will revolutionise this sector.

At the infrastructure level, the transition from preventive maintenance to a more targeted approach so-called predictive condition-based maintenance would dramatically alter this segment. Predictive maintenance strategies use sensors that continuously monitor crucial parameters and in conjunction with analysed historical trends evaluate the life-cycle stage of the monitored parts. This allows precisely predict impending failures and use the railway infrastructure with a higher efficiency, resulting in lower costs and enhanced safety. This paper describes one such system called RailCheck, developed and built at the Norwegian University of Science and Technology (NTNU). This system monitors railway infrastructure by utilising remote sensors and big-data analytics to interpret approaching and imminent threats hard to detect otherwise.

II. OVERALL RISKS & HAZARDS OVERVIEW

Train derailment and collisions are the most severe situations that may arise due to neglected maintenance and poor workmanship. They occur as a result of a number of distinct causes that can generally be classified as mechanical failure of track components (e.g. broken rails, cracked rails, broken gauge spreads), geometric failure of track components (e.g. rail climbing due to excessive wear, earthworks slip) and dynamic failure of train/track interaction (e.g. extreme hunting, vertical bounce, track shift under the train).

To prevent such events, railway tracks are regularly inspected by equipped measurement trains that use a combination of cameras and laser-based systems. These tools automatically evaluate the condition of the track and help identify mentioned faults before they can negatively affect performance or become a safety issue. Located problematic spots can then be manually inspected by the infrastructure managers (IMs) either from the camera footage or personally by the inspection in the field. This is a very convenient way how to effectively monitor and maintain this large and dense network. Unfortunately, most of these tools are limited just to the tracks, excluding points and level crossings (P&C), which have to be then still inspected solely manually. This in combination with a large number of these units, estimated to be one P&C per km of track (EU27) [8], makes the associated tolerable hazard rate (THR) difficult to maintain and demands for lower maintenance costs, believed to be an equivalent of about 0.3 km of the plain tracks [8], unable to achieve.

Stationary systems, as RailCheck, might be particularly helpful since they can be deployed on selected or remote objects that require more frequent or detailed surveillance. Long-term monitoring of key parameters of highly significant objects, such as endangered tracks, bridges, or P&C, would allow IMs to predict their response in time and react to sudden changes. These might be caused by insignificant random events as well as severe ones—e.g. floods, landslides or deliberate human actions. A reliable wireless sensor network (WSN) and classification algorithms are then the absolutely necessary to replace the regular inspections carried out today and fully transition from preventive to predictive condition-based maintenance. Due to the complexity of this system, only a monitoring part (WSN) will be further described.

III. SYSTEM DEFINITION & OPERATIONAL CONTEXT

RailCheck, shown in Fig. 1, is a dedicated condition-based maintenance system built over a three-year period as part of the DESTINATIONRAIL H2020 EU-project. It consists of multiple wireless battery-powered sensors (WS) attached directly to the rail body and a gateway (GW) located on the catenary mast along the rails. The GW communicates with the WS in range at sub-1GHz frequency and creates a local cell that forwards data to the server (SE), often referred to as a cloud. The train/track interaction is automatically captured by the WS's accelerometers, when the train passes over the infrastructure with deployed sensors. Data are then transmitted through a low-power wide-area network (LPWAN) to the SE, where these data are processed and analysed. IMs can thus get a detailed near real-time overview over their assets.

The system outlined above has been primarily developed to clarify and provide an answer as to whether or not the current state of the art allows the design of an optimal WSN for transition from preventive to predictive maintenance on such a large scale. Any answer must not only take into account a number of distinct parameters, including economic viability, system reliability, overall system security and safety, but also meet all project-specified requirements. These demanded low-cost battery-powered wireless sensors that are capable of monitoring selected infrastructure, e.g. railway P&C, for a time-span of more than 5 years. Results of these efforts were published in 2018 [9], and revealed the necessity of addressing also the safety-related parameters of this system. This manuscript aims to identify the necessary steps to make this system safe and deployable in real traffic conditions without losing any qualitative parameters of the system.

RailCheck was primarily intended to be used for monitoring the rails' geometric quality and their wear. However, due to the selected detection method used, many track-related data, including the train's response, is captured. This allows to observe the overall picture of the track structure, and to a certain extent the state of the passing trains. Several of the train chassis faults, e.g. flat wheel or axle bearing failure, can be identified at an early stage, which in turn prevents further damage to the rails. Modified sensors may be also used to monitor land slides and other highly critical events which further enhances this system's detection possibilities.

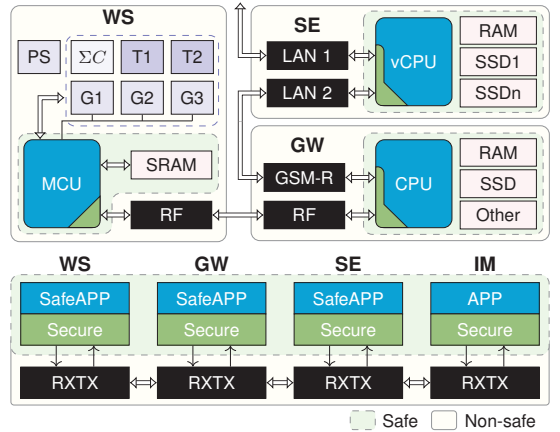


Fig. 1. RailCheck Schematic & Black Channel Concept

IV. DYSFUNCTIONAL ANALYSIS

The failure mode, effects and criticality analysis (FMECA) [10] were used to identify failure rates of different failure modes against the severity of their consequences while considering the barriers' effect. Please note that notation as A1 and F2 in Table I and in Fig. 2,3 represent the chapter in this section; B1 e.g. refer to the sub-chapter IV-B1.

A. WS Failures

The fundamental stress on low-cost and low-power consumption makes these sensors affordable and deployable on a mass scale. However, it is significantly more challenging to meet safety requirements and maintain expected reliability.

1) *Casing*: Housing failure, especially in the case of ingress protection (IP), may lead to several hazardous conditions. The battery might discharge in an undetected manner and a short-circuit may result in either a corrupted data or communication disruption. The same consequences may also include a moisture build-up inside the casing. These failures may be caused by random events such as poor workmanship, ageing of materials, exposure to excessive stress as well as by deliberate human actions such as vandalism.

2) *Electronic*: Hidden hardware/software (HW/SW) failures lead to severe catastrophic consequences that must be mitigated, optimally avoided completely. The sudden loss of power affecting large numbers of sensors, e.g. due to faulty updates, poses a real threat. The systematic failures are an even greater threat since they can hide the true condition of the monitored parts, and in certain cases remain undetected.

3) *Security*: Unauthorised physical manipulation is a severe threat since consequences of adversary actions can conceal true condition of the monitored parts. An adversary might try to gain knowledge by stealing one of the sensors from the remote areas. This would not go undetected, neither would it be prevented. Adversary would gain knowledge about the HW and could then try to reveal the SW installed on the WS. Adversary could learn about the defence measures in place and try to prevent triggering them the next time.

B. WS Barriers

Measures implemented to either prevent or mitigate the consequences of failures, identified in Section IV-A, are referred as barriers and are described in the following sub-chapters. The failure/barrier relationship, shown in Fig. 2,3, has been taken into account for the calculations in Section V.

1) *Displacement Detection*: The WS's vibration and movement are monitored by the 3-axis accelerometer that is most of the time set in a sleep measurement mode with a sampling frequency of 10 Hz. Any response over the selected threshold at any axis triggers the full measurement mode, allowing it to determine the source of this acceleration. Events are then classified based on their acceleration and wireless data. Identified safety-related events that differ from the train response, e.g. vandalism and unauthorised manipulation, are immediately reported to the system operator. All data provided after an identified unauthorised manipulation are treated as unreliable, and IM intervention is required.

2) *Physical Barrier*: The casing provides a passive barrier against deliberate and random failures A1 that may develop into liquid ingress A2, and a barrier against unauthorised manipulation A3. The casing is made of solid material PA2200 [11] containing acceptable material properties that include a high level of strength and firmness, strong chemical resistance, and excellent long-term stability. The Charpy impact strength, according to standard ISO 179/1eU [12], is a 53 kJ/m^2 which is expected to be sufficient to withstand most relevant impacts. Mechanical connections are protected by Acrylonitrile-Butadiene Rubber (NBR) o-ring sealings that might also be permanently sealed. The current casing is fitted with an unprotected dipole antenna that may be damaged and must be replaced with a build-in version covered by the casing. This casing will then be certified for IP mark IP64 according to the IEC 60529 [13].

3) *Reprogramming Lock*: WS's firmware is guarded by a code protection feature that locks in the device's reprogramming and reading its memory. In addition, the microcontroller's PCON register is monitored to identify sudden resets, reprogramming attempts or any other unexpected behaviour e.g. stack over-/underflow. The firmware is periodically verified to ensure the SW's integrity. The WS reacts to identified unauthorised manipulation by invalidating the cryptography keys on the GW and by erasing the WS memory. This prevents adversary from learning about defence mechanisms in place and becoming capable to gain access to the network.

4) *HW/SW Integrity*: To avoid data corruption originating from a sensor malfunction, hardware is equipped with multiple redundant sensors, as shown in Fig. 1. Temperature is measured by two sensors T1 and T2, acceleration by two or three accelerometers G1-3 measuring different magnitudes. First, this action increases the WS's usability, since WS can be deployed in various places and measures a wider range of accelerations. Secondly, it improves reliability, since the output values can be compared with one another to identify the corrupted data. This is performed directly by the microcontroller to prevent higher battery consumption caused by the additional wireless traffic. The microcontroller also

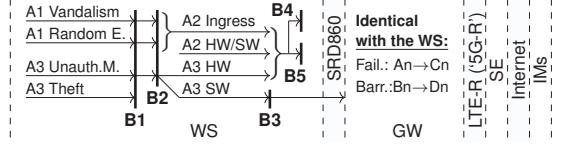


Fig. 2. HW/SW - Failures (An) & Barriers (Bn)

communicates with the peripherals strictly digitally, by the Serial Peripheral Interface (SPI), to prevent possible transmission errors or unauthorised manipulation. Communication error flags are monitored to detect any possible malfunctions. Self-diagnostics of the electronics are periodically performed to validate the calibration of the sensors and to detect defects.

5) *Power Supply*: Power diagnosis is an essential step to achieving reliable WS operation. The DC/DC converter with integrated coulomb counter, shown in Fig. 1 as ΣC , monitors the amount of power that has been used in order to estimate how much battery power is left. This allows the battery's entire life-cycle to be monitored with relative ease in order to prevent an unexpected power loss. The coulomb counter overflow, reach of the coulomb counter threshold and AC(ON) time overflow, which might indicate a low capacity of the built-in battery, are all supervised.

C. GW Failures

The GW is vulnerable to similar threats existing for a WS, as described in Section IV-A, but at the same time it can be better protected against deliberate and random threats. This is due to the possibility of attaching the casing to a less accessible location on a catenary mast along the rails, not as strict requirements for a low-cost and low-power consumption, and stricter requirements for overall security. If a GW gets compromised, all underlying infrastructure is affected, which jeopardises the whole local cell. This is caused by the fact that the higher we move towards the SE on the communication chain, the stronger the security must become in order to avoid larger and more severe consequences.

D. GW Barriers

The GW's failures/barriers model is in general identical to the one for WS shown in Fig. 2. What differs is the evaluation of frequency and severity for each failure that is seen in Table I and the way in which these barriers are implemented. These differences are summarised in following sub-chapters:

1) *Displacement Detection*: Detection is performed by the same means as for WS since this method provides accurate information about any atypical activity related to the casing.

2) *Physical Barrier*: The GW is enclosed in an industrial grade polycarbonate cabinet with an ingress protection rating IP66 (EN 60529) and impact resistance IK10 +35°C /IK08 -25°C (EN 62262). The door is protected by a key lock.

3) *Reprogramming lock*: The GW has a Linux distribution running on its HW that is responsible for both data consistency and overall data security. The data are stored in encrypted form, and access to the system is protected by the user password. GW uses Hypertext Transfer Protocol

Secure (HTTPS) requests to communicate with the SE and packet-based communication encrypted by an AES while communicating with the WS. All individual WS access keys to the network are securely stored in the GW's memory.

4) *HW/SW Integrity*: Barriers D3 and D4 from Fig. 2, identical to a B3 and B4 for a WS, are merged into a single barrier. This is described further above in Section IV-D3.

5) *Power Supply*: The GW is powered by a battery that is charged by a solar panel. To prevent sudden power loss, both the battery charging and power consumption are constantly monitored and optimised according to the current conditions.

E. Communication Failures

RailCheck uses the *black channel* concept, shown in Fig. 1, due to its favourable property that allows the use of unsecured public networks. This puts the RailCheck into Cat. 3 transmission system that must use strong countermeasures against the generic seven threats (G7T). These are known as (1) Repetition, (2) Deletion, (3) Insertion, (4) Re-sequencing, (5) Corruption, (6) Delay and (7) Masquerade. Moreover, EN 50159 describes 24 hazards, shown in Table A1 [14], that might lead to a communication failure. These 24 hazards are then classified into the G7T and must be prevented by well-known mechanisms *proven-in-use*. It is assumed that all threats except delay can be effectively prevented. The delay's severity is determined by its nature and how long it lasts:

1) *Temporary Outages*: These may be caused by randomly occurring environmental events, such as rain, lightning, solar radiation as well as by other electronic systems e.g. due to another active transmission on the same channel or another source of interference. These events are ranked as insignificant due to their temporary nature. It is not expected that these phenomena will result in outages longer than a couple of hours or days unless they simultaneously cause a partial or total traffic disruption. In these cases, the infrastructure would be physically monitored by other means.

2) *Long-term Outages*: These interruptions are labelled by severity category *critical* or *catastrophic*, due to their capacity to cause long-term outages. A typical attack comprises an entire spectrum jamming, which is a severe denial-of-service attack against wireless medium. It can be detected; however, it cannot be prevented. The source of interference must be actively tracked down and manually terminated.

F. Communication Barriers

Security events having direct consequences to a safety are handled in accordance with the 'Table 1 from EN 50159' [14]. The G7T from Section IV-E are then prevented by a combination of (1) cryptographic techniques, (2) safety code, (3) identification procedures, (4) feedback-messages, (5) source and destination identifiers, (6) timestamp, timeout and (7) sequence number. Since the *black channel* is used, packet creation and encryption must be performed already at the safe layer, which is in most cases implemented directly at the safe-microcontroller. The transmitter radio, shown in Fig. 1 as RXTX, then receives only cipher-text data. These cannot be manipulated and are simply forwarded to the communication channel. This so-called *end-to-end encryption*



Fig. 3. Communication Delay - Failures (En) & Barriers (Fn)

removes special requirements on hardware beyond the safety layer and simplifies the overall certification process.

In addition to the above mentioned mandatory mechanisms required by the standard, other methods are deployed at the endpoints and have a positive effect on transmission efficiency, battery life, resistance to random events. Indirectly, they have also a positive effect on overall security and safety. These measures are outlined in the following chapters:

1) *SRD860 (WS \Leftrightarrow GW)*: GW continuously monitors wireless communication on all channels and routes the communication with the WS over the most reliable set of links. Communication logs are aggregated at the SE for further analysis of any possible threats. Listen Before Talk (LBT), Adaptive Frequency Agility (AFA) and Adaptive Data Rate (ADR) controls are all used on both ends to achieve maximum permeability. In addition, WS is equipped with a simple algorithm monitoring the received signal strength indicator (RSSI). If the RSSI reaches the defined threshold, or WS loses its connection with the GW, WS sets the transmitting power to a maximum level of 10 dBm and lowers the transmitting data-rate down to a minimum value of 1 kbps. This is done in order to increase the the signal's transmission, thus increasing the link-budget. Afterwards, WS transmits the request to communicate over another set of frequencies. If a transmitted message stays unacknowledged on all channels, the device falls into a deep sleep mode to preserve the battery-life, having a scheduled wake-up call for another attempt. Communication attempts then decrease by factor 2 to a minimum period of one attempt every 12 hours.

2) *LTE-R or upcoming '5G-R' (GW \Leftrightarrow SE)*: Regardless which of these protocols are finally used, both of them will be adapted and certified for railway safety-critical communication and implemented in accordance with the EN 50159 up to the SIL 4. Both will also be operated by a railway wireless service provider in a licensed spectrum, which further lowers the probability of interference with other systems. Since these networks are assumed to be safe and secure, and will be used just as a service, no other measures are taken.

3) *Internet (SE \Leftrightarrow IMs)*: Communication with stakeholders is secured by the standard authentication and cryptographic protocols as they are used e.g. in communication with internet banking services. While this does not require a safe communication concept, communication must still remain secure. IMs establish the HTTPS connection with Transport Layer Security (\geq TLS 1.2) and are authorised by the two-step authentication process. IMs are then granted access based on their role in the system. Safe communication is not required since the IMs have no right to change the sensor data; indeed they are only allowed to display and evaluate these data. Due to internal procedures, their actions will not cause any dangerous situations to arise.

V. SAFETY INTEGRITY LEVEL (SIL) REQUIREMENTS

This section specifies how system requirements arising from previous chapters are allocated and elaborates analysis of system to be protected—railway P&C, and analysis of the monitoring system—RailCheck. While the condition-based maintenance system RailCheck is comprised of two parts; the monitoring part (WSN) and the big-data analytics, only the WSN part has been sufficiently developed to this moment.

A. Analysis of the System to be Protected—P&C

The vast majority of railway points today are equipped with a point machine—a device to remotely operate a turnout. This type of point must be protected by a safety function (SF), which puts the unit into a so-called *equipment under control* (EUC). Unacceptable risk arising from the EUC is handled by the SF responsible for achieving and maintaining the safe state. As regards turnout, SF 'SKF 2' [15] ensure that the railway point remains locked and provides the correct information about its position and status of locking. This function is part of the train's control and therefore part of the signalling system. RAMS requirements define seven hazards against which the point equipment must protect—(1) the wrong position, (2) the correct position with too much tolerance, (3) the correct position with missing locking, (4) accidental unlocking, (5) track width reduction, (6) track gauge expansion and (7) incorrect information on locking and positioning of the locking equipment. These hazards have an acceptable occurrence rate associated with the worst case scenario, train derailment, assigned to $THR=10^{-8}/h$ [15]. Assuming continuous operation, this is the equivalent of one failure per 1000 years and it is achieved by routine inspections, maintenance and by SFs. RailCheck's objective is to replace most of these inspections currently being performed on P&C by condition-based maintenance. RailCheck must therefore be at least as good as the traditional regular routine inspections carried out on P&C today.

To ensure the safety of this complex system, standards EN 50126, EN 50159 and IEC 61508 were examined and found to be relevant. Simultaneously, the EN 50128 and EN 50129 were assessed and excluded since they are more applicable for components that belong to signalling systems. RailCheck is an exclusive part of the maintenance system and will not play any direct role in the execution of the SFs.

B. Analysis of the Monitoring System—RailCheck (WSN)

The service life (SL) of rails is primarily determined by wear, plastic flow and defects. For example, wear mostly occurs on the gauge face in sections with high wheel-flanging forces e.g. when the train changes the track on a turnout. Certain wear is also caused by wheel/rail interaction on running surfaces due to maintenance activity, such as grinding. Plastic flow is a result of when wheel/rail contact stress exceeds the strength of the material. Rail defects happen due to many reasons and are a major concern. If they go undetected, they can grow and lead to unnecessarily expensive maintenance or, in a worst-case scenario, cause rail failure. Due to various improvements having been made

TABLE I
FMECA ANALYSIS

HW	Failure	Cause	S	FR _I	RRF					FR _F
					B1	B2	B3	B4	B5	
WS	A1 Casing	Vandalism Rand.Eve.	1	10 ⁻⁶	0.1	0.6	-	-	-	10 ⁻⁷
				10 ⁻⁷	0.6	0.1	-	-	-	10 ⁻⁸
	A2 Electronic	IP Failure HW/SW	2	10 ⁻⁷	+ incl.	-	0.1	0.1	10 ⁻⁹	
				10 ⁻⁸	-	-	0.1	0.1	10 ⁻¹⁰	
A3 Security	UM – HW UM – SW	2	10 ⁻⁹	0.1	0.6	-	0.1	0.1	10 ⁻¹²	
			10 ⁻⁹	0.1	0.9	0.1	-	-	10 ⁻¹¹	
		Theft	1	10 ⁻⁷	0.1	-	-	-	-	10 ⁻⁸
Wireless Medium SRD868	Long-term		3	10 ⁻¹⁰	-	-	-	-	-	10 ⁻¹⁰
GW	C1 Casing	Vandalism Rand.Eve.	1	10 ⁻⁸	0.1	0.1	-	-	-	10 ⁻¹⁰
				10 ⁻⁸	0.1	0.1	-	-	-	10 ⁻¹⁰
	C2 Electronic	IP Failure HW/SW	2	10 ⁻¹⁰	+ incl.	-	0.1	0.6	10 ⁻¹¹	
				10 ⁻⁸	-	-	0.1	0.6	10 ⁻¹⁰	
C3 Security	UM – HW UM – SW	3	10 ⁻⁸	0.1	0.9	-	0.1	0.9	10 ⁻¹¹	
			10 ⁻⁸	0.1	0.9	0.1	-	-	10 ⁻¹⁰	
		Theft	1	10 ⁻⁷	0.1	-	-	-	-	10 ⁻⁸
Wireless Medium GSM-R	Long-term		4		— Not Relevant —					
SE	Electronic Security	Unauth.M. HW Failure	4		— Not Relevant —					
	WAN Internet		3		— Not Relevant —					
IMs	Security	Unauth.M. HW Failure	1		— Not Relevant —					

HW (Hardware); **FR_I/FR_F** (FailureRate–Initial/Final) [h⁻¹]; **S** (Severity): 1–Insignificant, 2–Marginal, 3–Critical, 4–Catastrophic; **RRF** (RiskReductionFactor): 0.1–Most Likely Prevented, 0.3–Rather Prevented, 0.6–Rather Failed, 0.9–Most Likely Failed; **Assumptions** [n]: WS250k, GW5k, SE1; **UM** (Unauthorised Manip.) **Note**—Only relevant severe failures are stated.

to prolong rails' SL, the number of defects has in general increased [16]. All these factors negatively affect expected SL and in long-term undetected pose a threat to safety.

In order to calculate the values in Table I, THR must be properly stated. However, rail material has no specific SIL requirement and statistics records only track the failure rate on regularly inspected and maintained tracks. Moreover, there is no clear guidance given in either EN 5012x standards or technical regulations concerning THR assignment for condition-based monitoring systems. Discussions with contact personnel from the railway sector indicate that there are no internal guidelines on this topic, either. A majority of the systems used today are deployed as merely an additional monitoring step in regular inspections; therefore, safety-related parameters are not addressed. We have either not found any papers that take up whether or not condition-based maintenance should be assigned SIL requirements when it replaces routine inspections, or when inspections are extended to intervals so that defects may be expected during the period where only condition monitoring is available. As a result, current approaches to SIL allocation do not yet seem to be fully suited to these systems.

A review of other available technologies for condition-based monitoring suggest either no SIL requirement or SIL 1 to SIL 2. The systems using a SIL requirement are related to the monitoring of bearings for train wheels [17]. Our conclusion is that SIL requirement will be required at some point by IMs. Based on our review of current technologies,

a SIL 1 requirement for low-demand system as shown on Eq. 1 appears to be reasonable, as a design basis for a WS deployed on a single P&C, SIL 2 might then be achieved with redundancy by deploying several WSs on a single P&C.

$$THR = \left(\sum_{i=1}^n FR_{Fi} \right) < 10^{-4}/h \quad (SIL\ 1) \quad (1)$$

To estimate the failure rate by frequency of its occurrence for all failures from Table I, the following is assumed. Each national railway IM conducts its own RailCheck system, which defines the maximum number of WSs in the system. The European largest railway network, in Germany, comprises 44k km of railway tracks with an estimated one P&C per km of rails [8]. This equals an estimate of ~44k P&C, which are then each equipped with four WSs in case of railway turnout and by one or two WSs in case of level crossing. The system could therefore consist of ~250k units of WSs. The SL of WS is defined as a continuous operation 24 hours a day for an entire year over a time span of 10 years, which equals 87.6k hours. Next, to estimate the number of gateways in the system, we assume that there is on average one gateway per 50 WSs, which produces ~5k GWs. So e.g., the initial failure rate (FR_I) for failure A2 Ingress is calculated assuming that <2.5% of all WSs fails during SL due to IP failure:

$$FR_I = \frac{Failures}{SL \times Units} = \frac{6k}{87.6k \times 250k} = 2.74 \times 10^{-7} \quad (2)$$

For estimations of the final failure rate (FR_F) after the effect of barriers, FR_I is multiplied by the risk reduction factor (RRF), which reflects the effect of each independent barrier.

$$FR_F = FR_I \times RRF = 274n \times 0.1 \times 0.1 = 2.74 \times 10^{-9} \quad (3)$$

An analysis of the entire communication chain has been excluded, since well known mechanisms *proven-in-use* are already in place. This analysis has primarily focused on custom-made and physically exposed units—WSs and GWs.

VI. CONCLUSION

The transition from wired to wireless communication is an overall trend in all areas of human activity. In the railway domain, this was defined already in the early 90s by setting up the working group on GSM-R as a result of work on ETCS. While the main motivation was to resolve interoperability across the national safety systems incompatible over the borders, it is inevitable that next-generation railway networks will moreover to the current state also incorporate a public data transmissions. Communication with the rolling stock, safety-critical infrastructure and other non-safety related systems will then all coexist under one common roof. This will allow safe connections with trains and turnouts, transmit camera surveillance streams from trains and stations and provide passengers WiFi while travelling. This will positively affect a whole range of current and impending applications and it will allow new sustainable deployments, including the emergence of smart-points—a turnout capable of utilising next-generation communication networks such as LTE-R or '5G-R', and accommodate additional applications. This will

minimise the overall costs of systems like RailCheck so they will no longer represent any significant costs even for mass-scale deployments. Until then, RailCheck can be used for (1) remote monitoring of selected turnouts requiring additional surveillance and (2) as a multi-purpose platform for developing robust algorithms for condition-based maintenance.

This paper has demonstrated a certain number of the initial steps required for applying IEC 61508, EN 50126 and EN 50159. Emphasis was placed on clarifying the context of use, potential hazards and SIL requirements that might apply to this system. In addition, an initial dysfunctional analysis has been made to justify the idea that it seems possible to meet the suggested SIL requirements with respect to systematic and random HW failures. However, further work should include a more detailed analysis of both failure rate estimates as well as other measures that are imposed by the SIL requirements. For instance on the avoidance and control of SW faults in the development of the application program. This paper has also reviewed ways to consider security along with safety design. The exposure of such a system due to wireless technology and devices that may be accessed by anyone entering the tracks means that no such system will be safe if it is also not secure.

REFERENCES

- [1] European Commission. *Delivering an effective and interoperable European Rail Traffic Management System (ERTMS)-the way ahead*. SWD(2017) 375 final. EU, 2017.
- [2] European Commission. *ERTMS—Delivering Flexible and Reliable Rail Traffic*. EU, 2006. ISBN:92-79-00584-7.
- [3] EIRENE-GSM-R Functional Group. *Functional Requirements Specification Version 8.0.0*. UIC, 2012. ISBN:2-7461-1831-7.
- [4] EIRENE-GSM-R Operators Group. *System Requirements Specification Version 16.0.0*. UIC, 2012. ISBN:2-7461-1832-4.
- [5] IEC. IEC 61508:2010—Functional safety of E/E/PE safety-related systems. *International Standards and Conformity Assessment for all electrical, electronic and related technologies*, 2010.
- [6] K. Guan, Z. Zhong, and B. Ai. Assessment of LTE-R Using High Speed Railway Channel Model. In *Third International Conference on Communications and Mobile Computing*, pages 461–464, 2011.
- [7] ERTMS Benefits. http://www.ertms.net/?page_id=44. Acc.: 2019-02.
- [8] Capacity for Rail (C4R). *Operational failure modes of Switches and Crossings*. C4R, 2015. Public deliverable—'D1.3.1'.
- [9] J. Sramota and A. Skavhaug. RailCheck: A WSN-Based System for Condition Monitoring of Railway Infrastructure. In *21st Euromicro Conference on Digital System Design (DSD)*, pages 347–351, 2018.
- [10] IEC 60812:2018 - Failure modes and effects analysis (FMEA and FMECA). <https://www.standard.no/no/Nettbutikk/produktkatalogen/Produktpresentasjon/?ProductID=988328>. Accessed: 2019-02-04.
- [11] Material Data sheet - PA2200. http://www.shapeways.com/topics/udesign/materials/white-strong-flexible/pa2200_material_data_sheet_12.08_en...pdf. Accessed: 2019-02-04.
- [12] ISO 179-1:2010 - Plastics - Determination of Charpy impact properties. <http://www.standard.no/no/Nettbutikk/produktkatalogen/Produktpresentasjon/?ProductID=432313>. Accessed: 2019-01-30.
- [13] IEC 60529:1989 - Degrees of protection provided by enclosures (IP Code). <http://www.standard.no/no/Nettbutikk/produktkatalogen/Produktpresentasjon/?ProductID=658451>. Accessed: 2019-01-30.
- [14] CENELEC. EN 50159:2010 - Safety-related communication in transmission systems. *Official Journal of the European Union*, 2010.
- [15] BaneNOR. Signal/Projektering/Sporveksel og sporsperreutrustning. https://trv.banenor.no/wiki/Signal/Projektering/Sporveksel-og-sporsperreutrustning#RAMS-1_krav. Accessed: 2019-03-05.
- [16] NSW. TMC227-Surface Defects in Rails. https://www.transport.nsw.gov.au/system/files/media/asa_standards/2017/tmc-227.pdf. Acc: 2019.
- [17] SKF. Bogie condition monitoring - Extract from the Railway technical handbook, volume 1, chapter 8, page 152 to 163. <https://www.skf.com/binary/12-62755/RTB-1-08-Bogie/index.html>. Accessed: 2019-04-02.

Paper A.3

RailCheck Dataset of Vehicle-Track Interaction Measured on Railway Turnouts

This paper is awaiting publication and is not included in NTNU Open

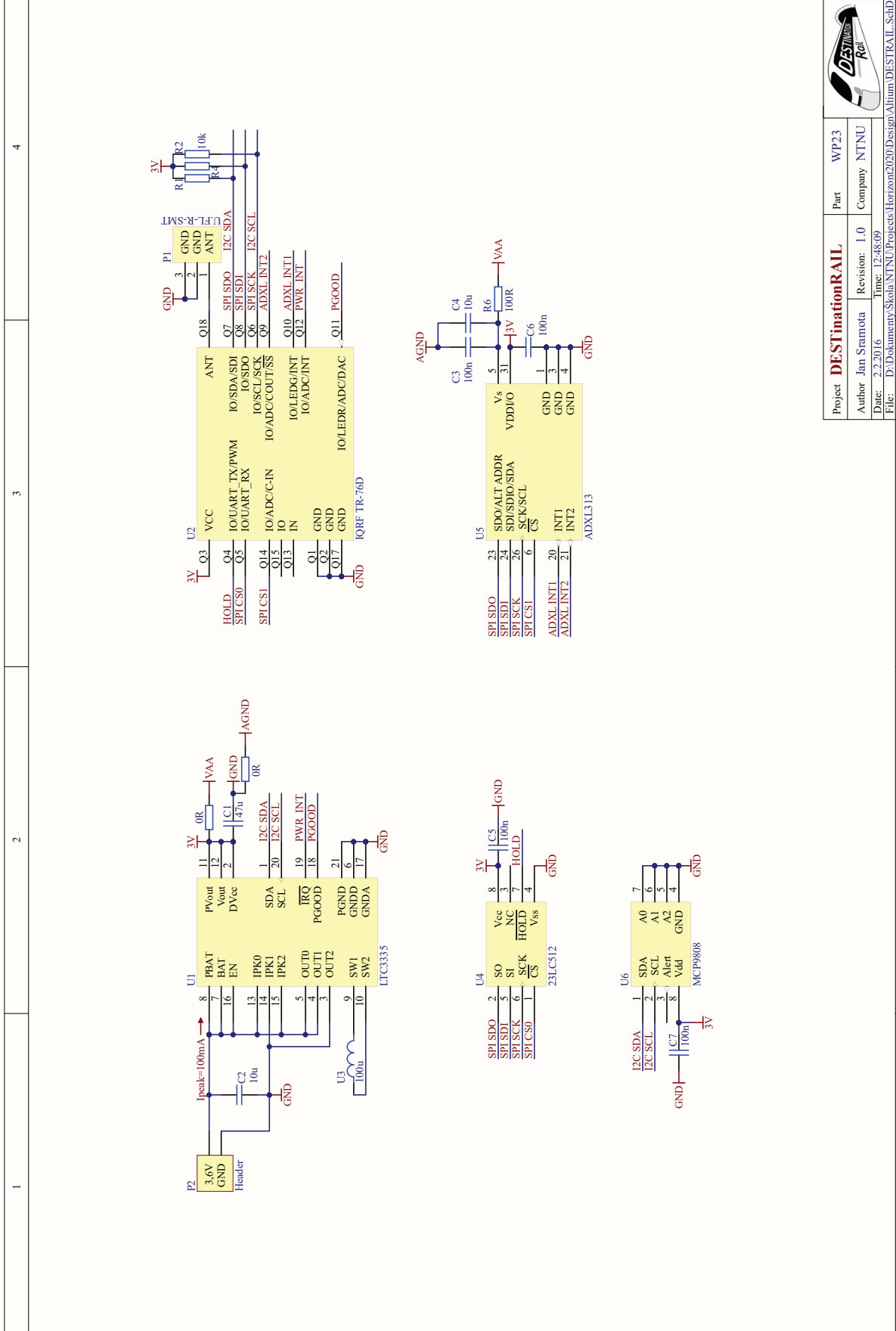
Appendix B

Schematic

Schematic B.1

Wireless Sensor Hardware v1.0

A B C D



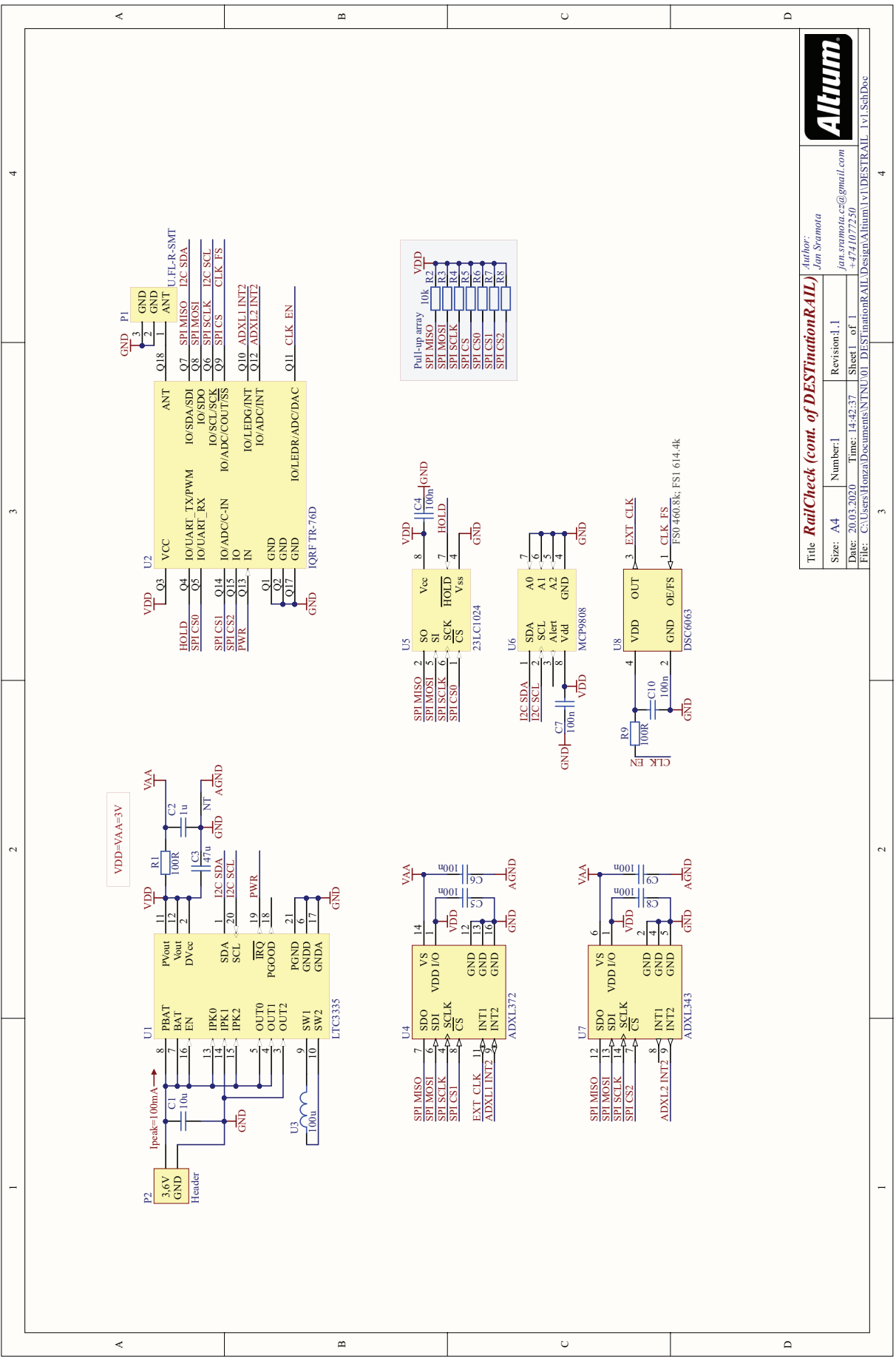
A B C D

1 2 3 4

Project	DESTINATION RAIL	Part	WP2.3
Author	Jan Stramota	Revision:	1.0
Date:	2.2.2016	Time:	12:48:09
File:	D:\Dokumenty\Skolai\NTNU\Projects\Horizon2020\Design\Altium\DESTINATION_RAIL_SchDoc		

Schematic B.2

Wireless Sensor Hardware v1.1



A
B
C
D

1
2
3
4

A
B
C
D

1
2
3
4

RailCheck (cont. of DESTINATIONRAIL)

Author: Jan Sramota

Size: A4	Number: 1	Revision: 1.1
Date: 20.03.2020	Time: 14:42:37	Sheet 1 of 1
File: C:\Users\Honza\Documents\INTNU\01_DESTINATIONRAIL_V1\DESTRAIL_V1_SchDoc		

Altium

Schematic B.3

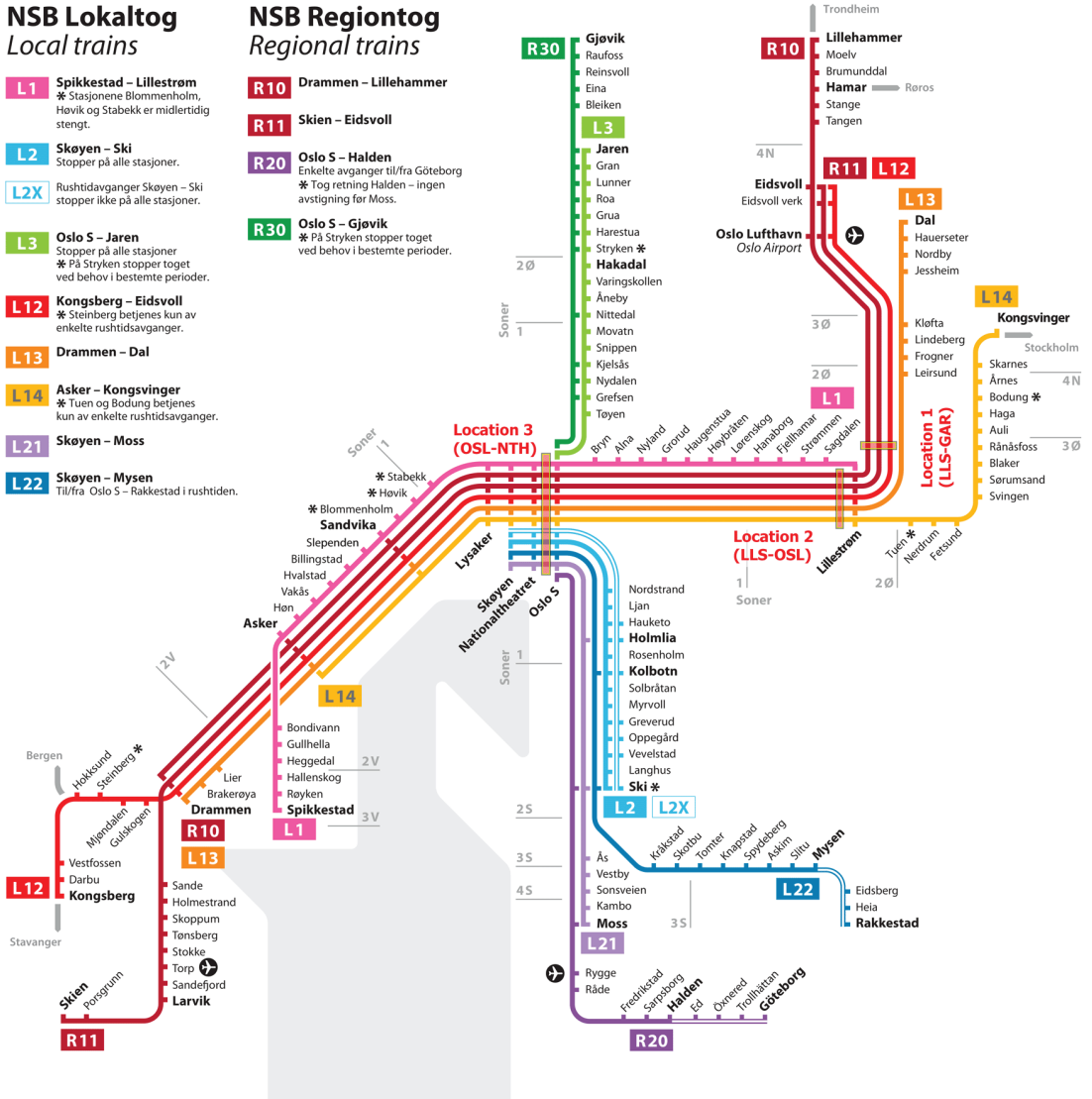
Norwegian Railway Network

NSB Lokaltog Local trains

- L1** Spikkestad – Lillestrøm
* Stasjonene Blommenholm, Hovik og Stabekk er midlertidig stengt.
- L2** Skøyen – Ski
Stopper på alle stasjoner.
- L2X** Rushtidavganger Skøyen – Ski
stopper ikke på alle stasjoner.
- L3** Oslo S – Jaren
Stopper på alle stasjoner
* På Stryken stopper toget ved behov i bestemte perioder.
- L12** Kongsberg – Eidsvoll
* Steinberg betjenes kun av enkelte rushtidsavganger.
- L13** Drammen – Dal
- L14** Asker – Kongsvinger
* Tuen og Bodung betjenes kun av enkelte rushtidsavganger.
- L21** Skøyen – Moss
- L22** Skøyen – Mysen
Til/fra Oslo S – Rakkestad i rushtiden.

NSB Regiontog Regional trains

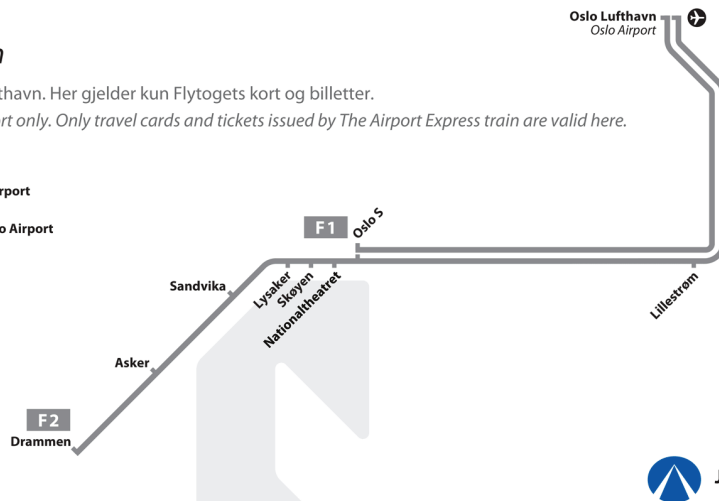
- R10** Drammen – Lillehammer
- R11** Skien – Eidsvoll
- R20** Oslo S – Halden
Enkelte avganger til/fra Göteborg
* Tog retning Halden – ingen avstigning for Moss.
- R30** Oslo S – Gjøvik
* På Stryken stopper toget ved behov i bestemte perioder.



Flytoget Airport Express Train

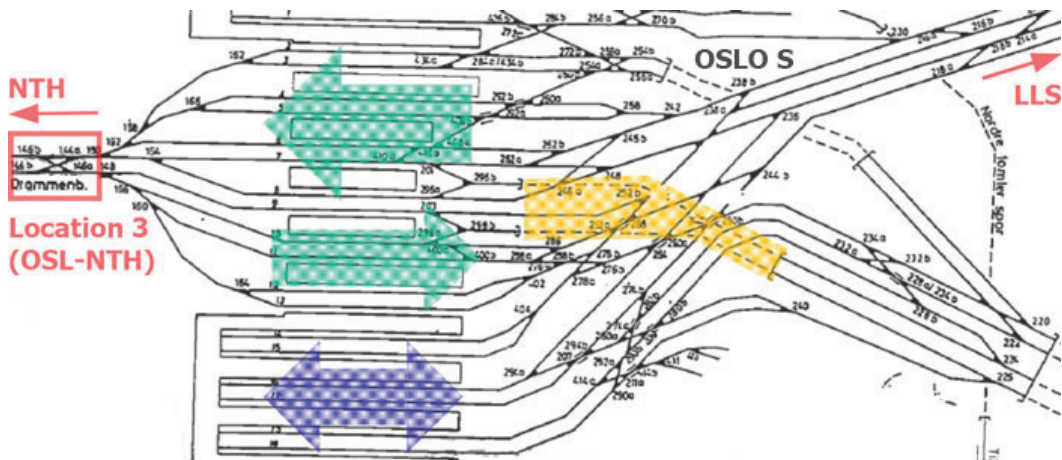
Kun for reiser til og fra Oslo Lufthavn. Her gjelder kun Flytogets kort og billetter.
For travel to and from Oslo Airport only. Only travel cards and tickets issued by The Airport Express train are valid here.

- F1** Oslo S – Oslo Lufthavn / Oslo Airport
Direkte
- F2** Drammen – Oslo Lufthavn / Oslo Airport
Stopper på alle Flytogstasjoner



Schematic B.4

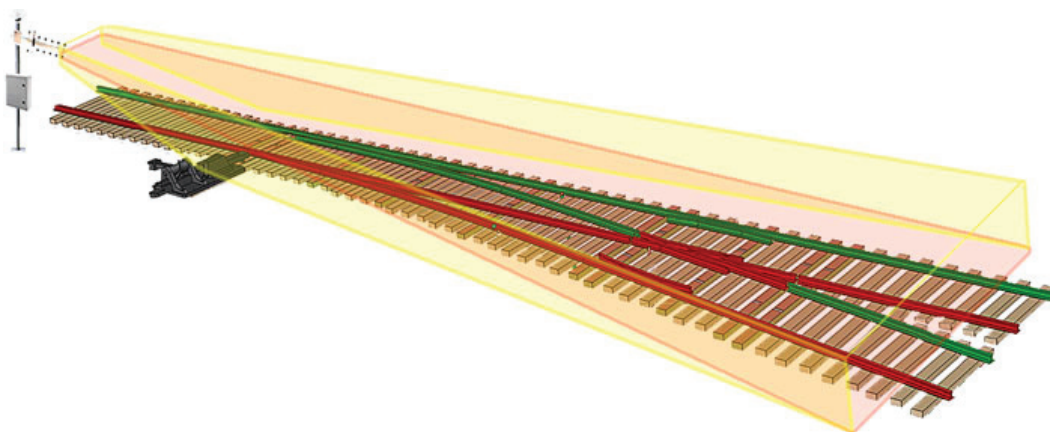
Various Amendments



(a) Measuring location 3 (OSL-NTH)



(b) Typical locations for a WS installation (P1, P3 and P4 may be in one line)



(c) Gateway v1.1 coverage (used in Germany)

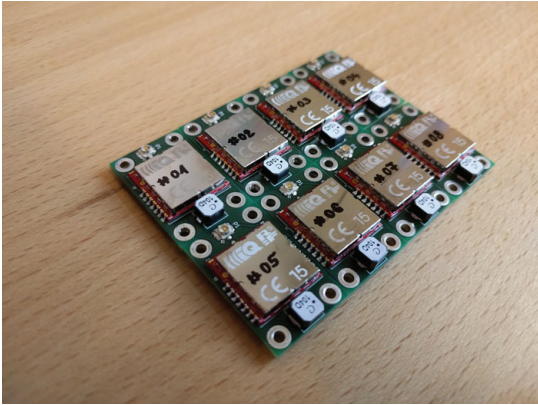
Figure B.1: Various amendments

Appendix C

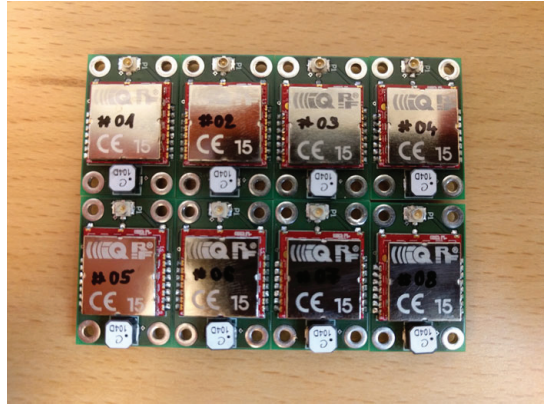
Photos

Photo C.1

Wireless Sensor (PCB, WSC)



(a) WS PCB v1.0 (Top, view 1)

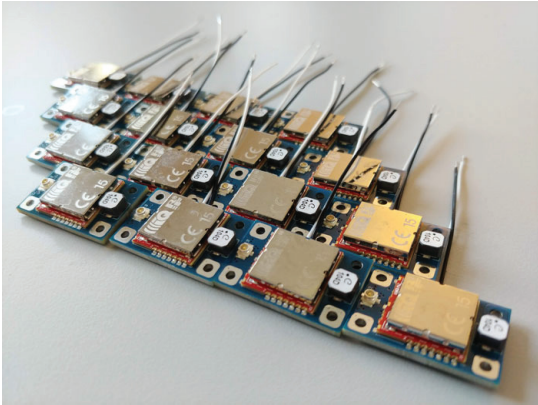


(b) WS PCB v1.0 (Top, view 2)

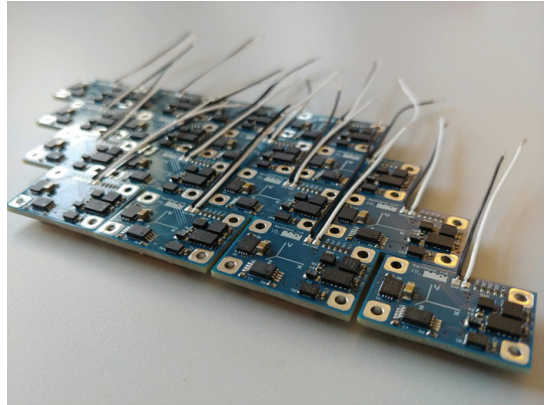


(c) WSC v1.0

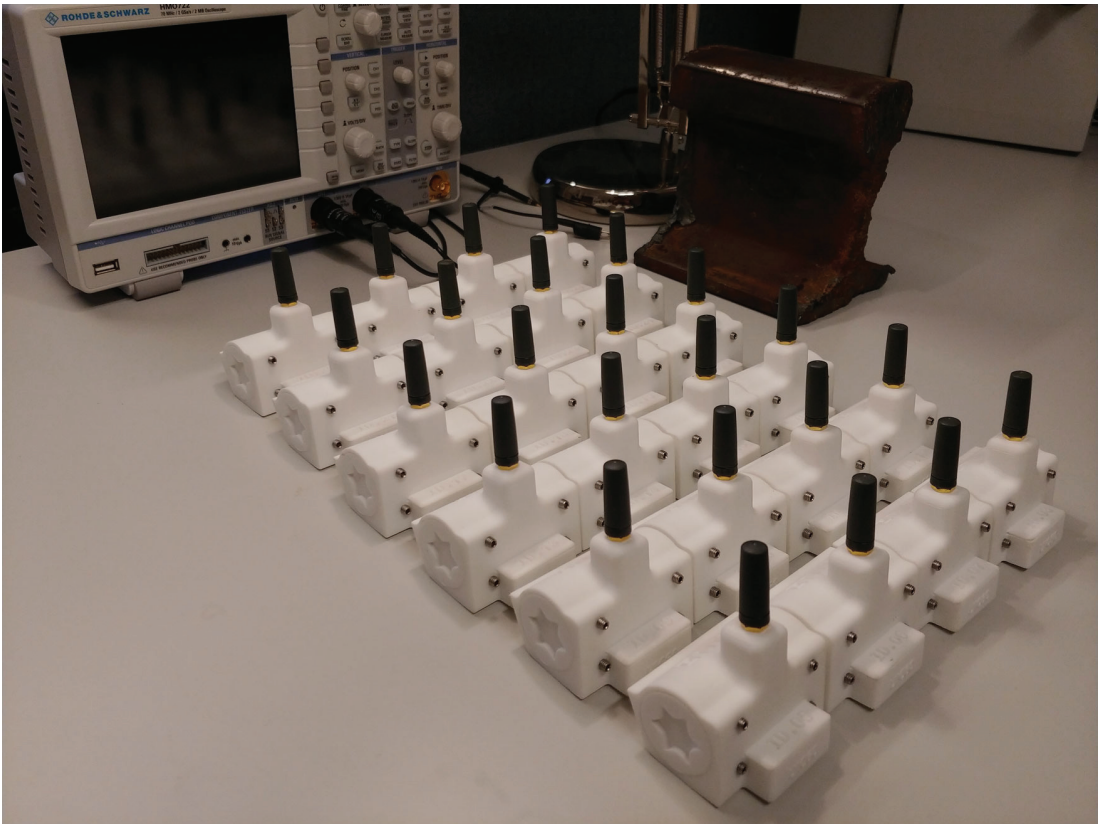
Figure C.1: Wireless sensor v1.0



(a) WS PCB v1.1 (Top)



(b) WS PCB v1.1 (Bottom)



(c) WSC v1.1

Figure C.2: Wireless sensor v1.1

Photo C.2

Content Management System (CMS)

Hello XSramik [Log out](#)

[Dashboard](#) [Content](#) [Structure](#) [Appearance](#) [People](#) [Modules](#) [Configuration](#) [Reports](#) [Help](#)

Edit shortcuts
Add content Find content Performance

DESTINATION RAIL Monitoring

Home
My account [Log out](#)

Home

Q

Navigation

- ▼ DESTINATION RAIL
 - Monitoring
 - Locations
 - Reference data
 - Sensors
- Add content

Who's online

There are currently 0 users online.

Switch user

- XSramik
- DEV
- TUM

Data ID416

Data record

id	nid	gid	[kB]	[sec]	T _{WT}	T _{WL}	T _L	T _{RM}	T _{MM}	captured by sensor	links
416	5	101	150	4.0	13.2 m	6.3 m	57 s	6 s	20.6 m	29-06-2017 15:45:55	↶ ↷

Graph ID_416

Time record

Wait for train	T _{MeasMode} ~ T _{TrainPassed}	15:29:32 ~ 15:42:46	13.2 m
Wait for link	T _{TrainPassed} ~ T _{SendData}	15:42:46 ~ 15:49:05	6.3 m
Link time (RF TX data)	T _{SendData} ~ T _{AllReceived}	15:49:05 ~ 15:50:02	57 s
LinkEnd to MeasMode	T _{AllReceived} ~ T _{MeasModeText}	15:50:02 ~ 15:50:08	6 s
MeasMode to MeasMode	T _{MeasMode} ~ T _{MeasModeText}	15:29:32 ~ 15:50:08	20.6 m

Log record

[DATA-ID_416] There are 50 records between rows ID45580 and ID45690.

id	dir	nid	cmd	msg	updated	description
45580	TX	00	A0	00	29/06/2017 15:29:32	[ALL] Command-> MEASURE MODE!
45584	RX	05	A0	00	29/06/2017 15:29:32	[05] Waiting for train. (RF disabled)
45585	RX	05	A0	FF	29/06/2017 15:42:46	[05] Train just passed. data captured!
45589	TX	00	C0	00	29/06/2017 15:43:34	[ALL] Command-> GET STATUS!
45593	RX	05	A0	4FD	29/06/2017 15:43:35	[05] Waiting to transmit 1277 packets!
45601	TX	FF	01	00	29/06/2017 15:45:47	[GW] SPI GET -> Perifery Switch
45602	TX	00	C0	00	29/06/2017 15:45:54	[ALL] Command-> GET STATUS!
45603	TX	FF	01	00	29/06/2017 15:45:48	[GW] SPI GET -> Perifery Switch
45606	TX	00	C3	00	29/06/2017 15:45:50	[ALL] Command-> GET firmware version!
45608	RX	05	A0	4FD	29/06/2017 15:45:55	[05] Waiting to transmit 1277 packets!
45620	TX	05	B0	00	29/06/2017 15:49:00	[05] Command-> SEND DATA!
45625	TX	05	B0	00	29/06/2017 15:49:05	[05] Command-> SEND DATA!
45626	RX	05	B0	4FD	29/06/2017 15:49:05	[05] Transferring data began! (1277 packets)
45627	RX	05	B0	FF	29/06/2017 15:49:59	[05] Transferring data ended!
45628	TX	05	B1	00	29/06/2017 15:50:00	[05] Command-> RE-SEND LOST PACKETS!
45629	RX	05	B0	FF	29/06/2017 15:50:00	[05] Transferring data ended!
45630	TX	05	B2	00	29/06/2017 15:50:02	[05] Command-> ALL DATA RECEIVED!

Powered by [Drupal](#)

Figure C.3: CMS v1.0—Train record

Monitoring of Railway Turnouts



- Home
- Data
- Network
- Scheduler
- Dataset
- Registration
- Contact

Environment Switch

Measure	Standby
Live	Dev
Full	Restricted

Console

-- Commands --

-- Turnout --

01	02	03	04	05	06	07	08	09	10
11	12	13	14	15	16	17	18	19	20
21	22	23	24	25	26	27	28		

Send

- Tools
- Data
 - Network
 - Scheduler
 - DB Tables
 - Add content

Who's online

There are currently 1 users online.

XStramik

Who's new

Andri

zudeke@banenor.no

Cinman

XStramik

Render Graph

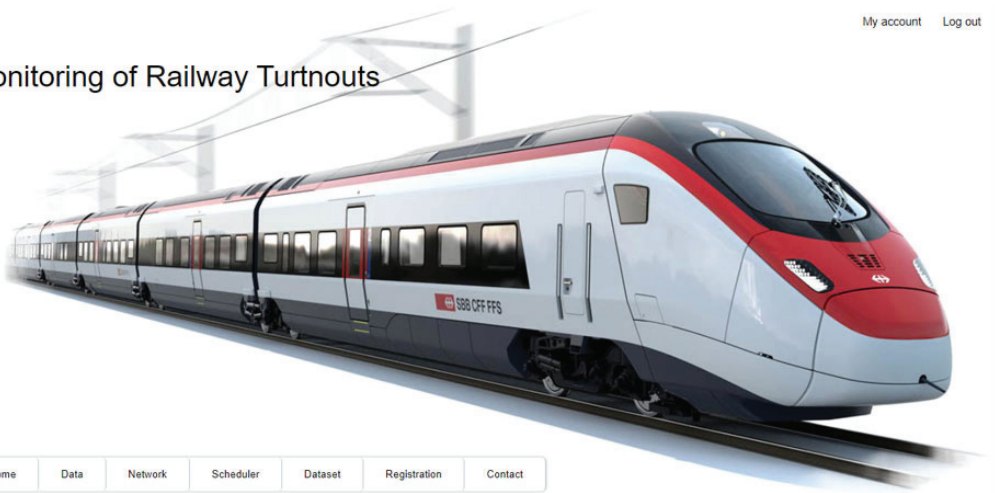


Powered by ZingChart

Parameters	Communication Log	Location
General Info		
Parameter	Value	Measurement Info
DB ID	1940	Accelerometer
VehicleAlias	Train 3	Lossless Compression
VehicleType	Not implemented	External Clock
[NID] Node ID (dec)	27	Output Data Rate
[NID] Node ID (hex)	0x1B	Bandwidth
[MID] Module ID (Unique Node Serial)	0x811180E2	Low Noise
[GID] Gateway ID	GESC94700YH7	WakeUp Rate
[LID] Location ID	133	Filter Settle
APP Version	v1.08	Low Pass Filter
Ambient Temperature	2.5°C	High Pass Filter
Power Consumed (Total)	1250 mAh (16%)	Activity Threshold (Y-axis)
Packets Transmitted	1333 (0x513)	Inactivity Threshold (Y-axis)
Packets to Stop	1332 (0x514)	Activity Timer
Packets Available	1347 (0x543)	Inactivity Timer
Days Since Beginning of Recording	208	Inactivity Samples (Y-axis)
Publicly Restricted Info		
Parameter	Value	
VehicleRef	(Confidential - removed before print screen)	
Train Details (line, from (platform) -> to)	(Confidential - removed before print screen)	
Measured RAW Data	0160FFB0FC70...	
OS Version (Build)	4.030 (08C8)	
TR Series	11	
FCC	0	
MCU Type	4	
Data Size	79.98 kB	
DB Updated	(Confidential - removed before print screen)	
DB Record Created	(Confidential - removed before print screen)	

Figure C.4: CMS v1.1—Train record

Monitoring of Railway Turnouts



Home Data Network Scheduler Dataset Registration Contact

Environment Switch

Measure	Standby
Live	Dev
Full	Restricted

Console

-- Commands --

-Turnout- FF

01 02 03 04 05 06 07 08 09
10 11 12 13 14 15 16 17 18
19 20 21 22 23 24 25 26 27

Send

Tools

- [Data](#)
- [Network](#)
- [Scheduler](#)
- [DB Tables](#)
- [Add content](#)

Who's online

There are currently 1 users online.
[XSramik](#)

Who's new

- [André](#)
- [andeke@banenor.no](#)
- [Cimrman](#)
- [XSramik](#)

Train Find

Monitor Find List

StationRef OperatorRef LineRef DirectionRef

LLS [] R10 [] [] [] Search Show Map

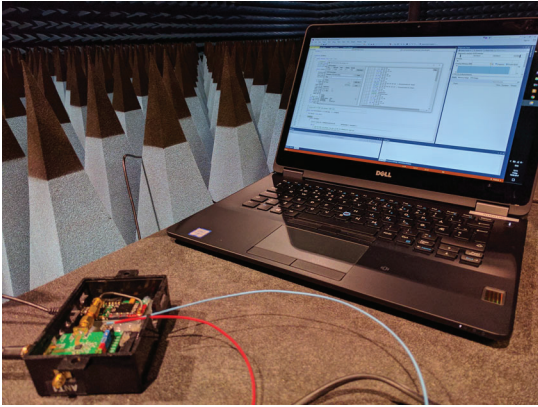
#	VehicleRef	Line	OriginRef	DestinationRef	ORIG -- MON -- DEST	Platform	
<input type="checkbox"/>	1	304	R10	LHM (3)	DRM (1)	05:25 -- 07:16 -- 08:02	1
<input type="checkbox"/>	2	307	R10	DRM (1)	LHM (3)	06:57 -- 07:45 -- 09:37	4
<input type="checkbox"/>	3	308	R10	LHM (1)	DRM (1)	07:14 -- 09:16 -- 10:02	1
<input type="checkbox"/>	4	311	R10	DRM (1)	LHM (3)	08:57 -- 09:45 -- 11:40	4
<input type="checkbox"/>	5	312	R10	LHM (1)	DRM (1)	09:07 -- 11:16 -- 12:02	1
<input type="checkbox"/>	6	315	R10	DRM (1)	LHM (3)	10:57 -- 11:45 -- 13:41	4
<input type="checkbox"/>	7	316	R10	LHM (3)	DRM (1)	11:14 -- 13:16 -- 14:02	1
<input type="checkbox"/>	8	319	R10	DRM (1)	LHM (3)	12:57 -- 13:45 -- 15:37	4
<input checked="" type="checkbox"/>	9	336	R10	LHM	DRM	12:57 -- 13:45 -- 15:37	4
<input type="checkbox"/>	10	318	R10	LHM (3)	DRM (1)	12:08 -- 14:16 -- 15:02	1
<input type="checkbox"/>	11	321	R10	DRM (1)	LHM (3)	13:57 -- 14:45 -- 16:44	4
<input type="checkbox"/>	12	320	R10	LHM (3)	DRM (1)	13:10 -- 15:16 -- 16:02	1
<input type="checkbox"/>	13	323	R10	DRM (1)	LHM (3)	14:57 -- 15:45 -- 17:37	3
<input type="checkbox"/>	14	322	R10	LHM (3)	DRM (1)	14:11 -- 16:16 -- 17:02	1
<input type="checkbox"/>	15	325	R10	DRM (1)	LHM (3)	15:57 -- 16:45 -- 18:41	4
<input type="checkbox"/>	16	324	R10	LHM (1)	DRM (1)	15:07 -- 17:16 -- 18:02	1
<input checked="" type="checkbox"/>	17	327	R10	DRM (1)	LHM (3)	16:57 -- 17:45 -- 19:40	4
<input checked="" type="checkbox"/>	18	326	R10	LHM (3)	DRM (1)	16:14 -- 18:16 -- 19:02	1
<input type="checkbox"/>	19	328	R10	LHM (1)	DRM (1)	17:07 -- 19:16 -- 20:02	1
<input type="checkbox"/>	20	331	R10	DRM (1)	LHM (3)	18:57 -- 19:45 -- 21:41	3
<input type="checkbox"/>	21	330	R10	LHM (3)	DRM (1)	18:11 -- 20:16 -- 21:02	1

Monitor

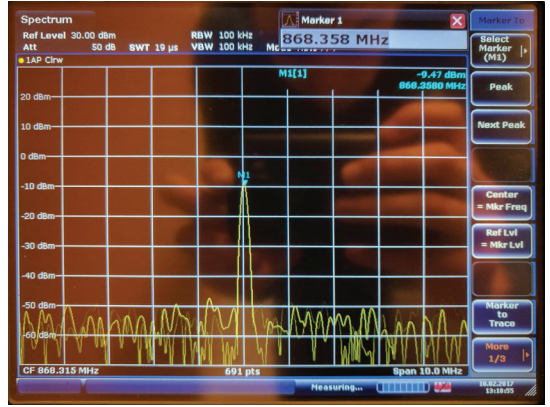
Figure C.5: CMS v1.1—Monitoring scheduler

Photo C.3

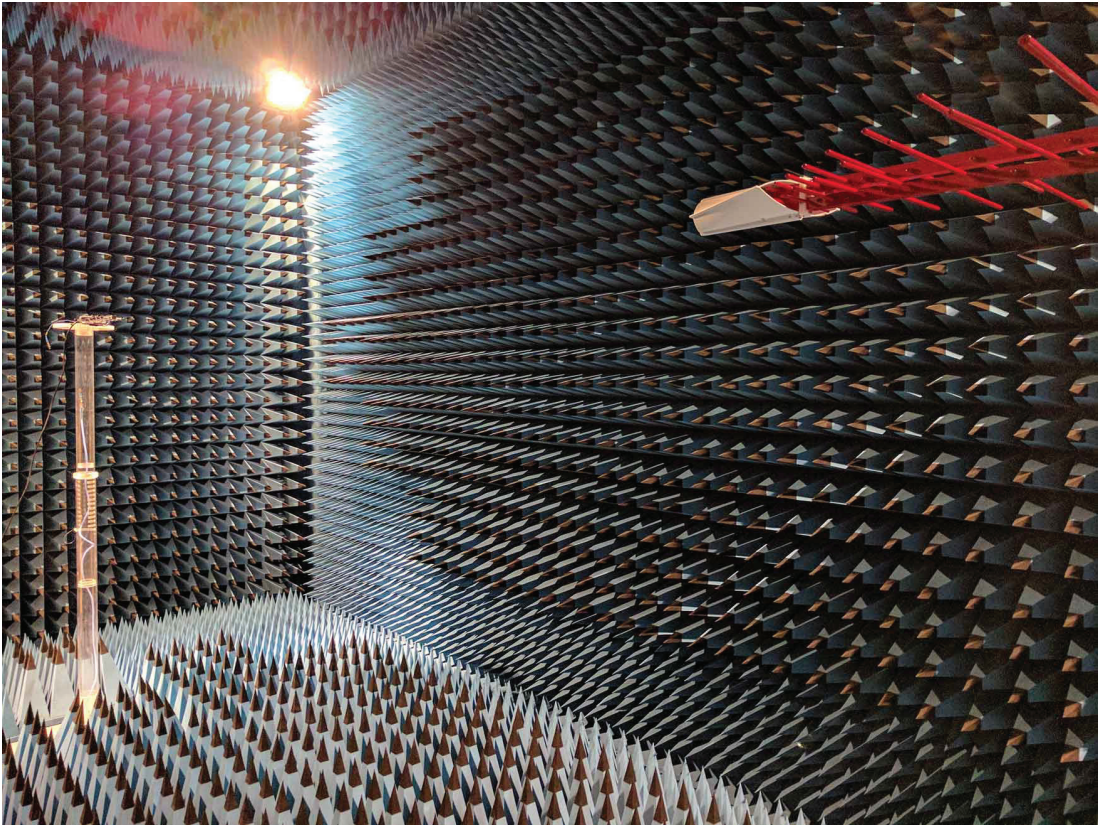
Antenna Test



(a) Preparations for measurements



(b) Signal measured on the reference antenna



(c) Anechoic chamber overview

Figure C.6: Antenna test

Photo C.4

Coverage Test



(a) Gateway location (view 1)



(b) Gateway location (view 2)



(c) Mutual position of the gateway and the wireless sensors

Figure C.7: Coverage test: gateway



(a) Location 1—WS detail



(b) Location 2—WS detail



(c) Location 1—WS during snow test



(d) Location 2—WS during snow test



(e) Location 1—WS—GW overview



(f) Location 2—WS—GW overview

Figure C.8: Coverage test: wireless sensors

Photo C.5

Measurement Denmark



(a) Beginning of the railway turnout



(b) Oncoming passenger train



(c) Testing communication of the wireless sensor

Figure C.9: Measurements in Denmark (1)



(a) Wireless sensor (view 1)

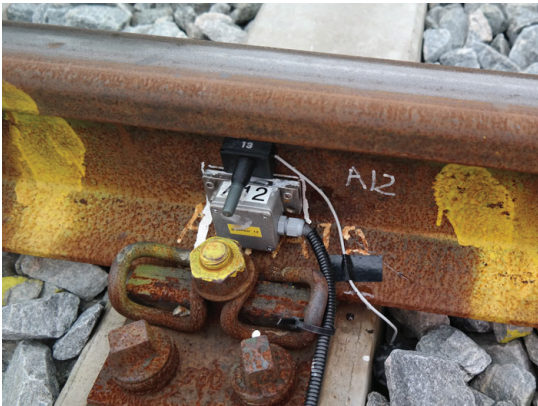


(b) Oncoming steam locomotive



(c) Wireless sensor (view 2)

Figure C.10: Measurements in Denmark (2)



(a) WS on the rail-web (detail)



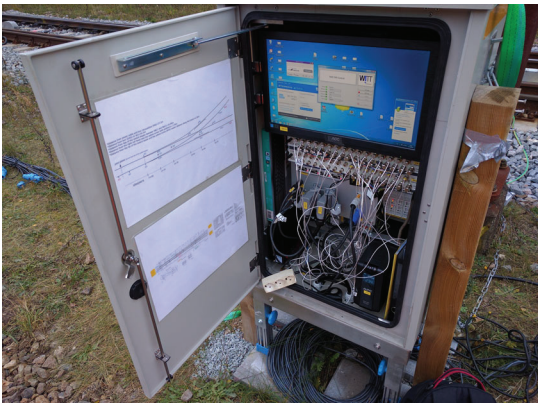
(b) WS on the rail-web (overview)



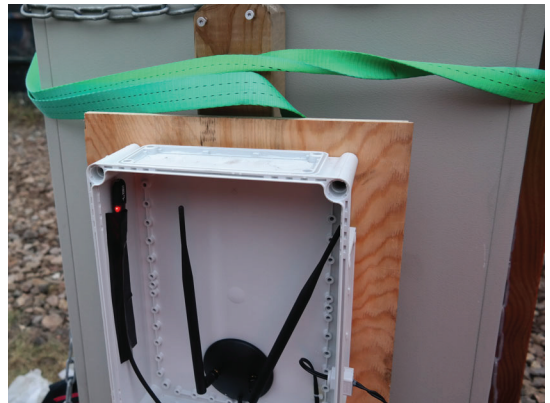
(c) WS on the sleeper (detail)



(d) WS on the sleeper (overview)



(e) Gateway's cabinet



(f) Gateway's antenna casing

Figure C.11: Measurements in Denmark (3)

Photo C.6

Measurement Germany



(a) Rail-web location



(b) Railway sleeper location



(c) Wireless sensors (overview)

Figure C.12: Measurements in Germany (1)



(a) Rail overview



(b) Sleeper overview



(c) Gateway overview

Figure C.13: Measurements in Germany (2)

Photo C.7

Measurement Oslo



(a) Location 1 (GAR-LLS)



(b) Location 2 (LLS-OSL)



(c) Location 3 (OSL-NTH)

Figure C.14: Measurements in Norway (1)



(a) WSC v1.1 attached to a rail-web



(b) Gateway v1.1 (3 units)



(c) LLS-OSL location (opposite direction view)

Figure C.15: Measurements in Norway (2)

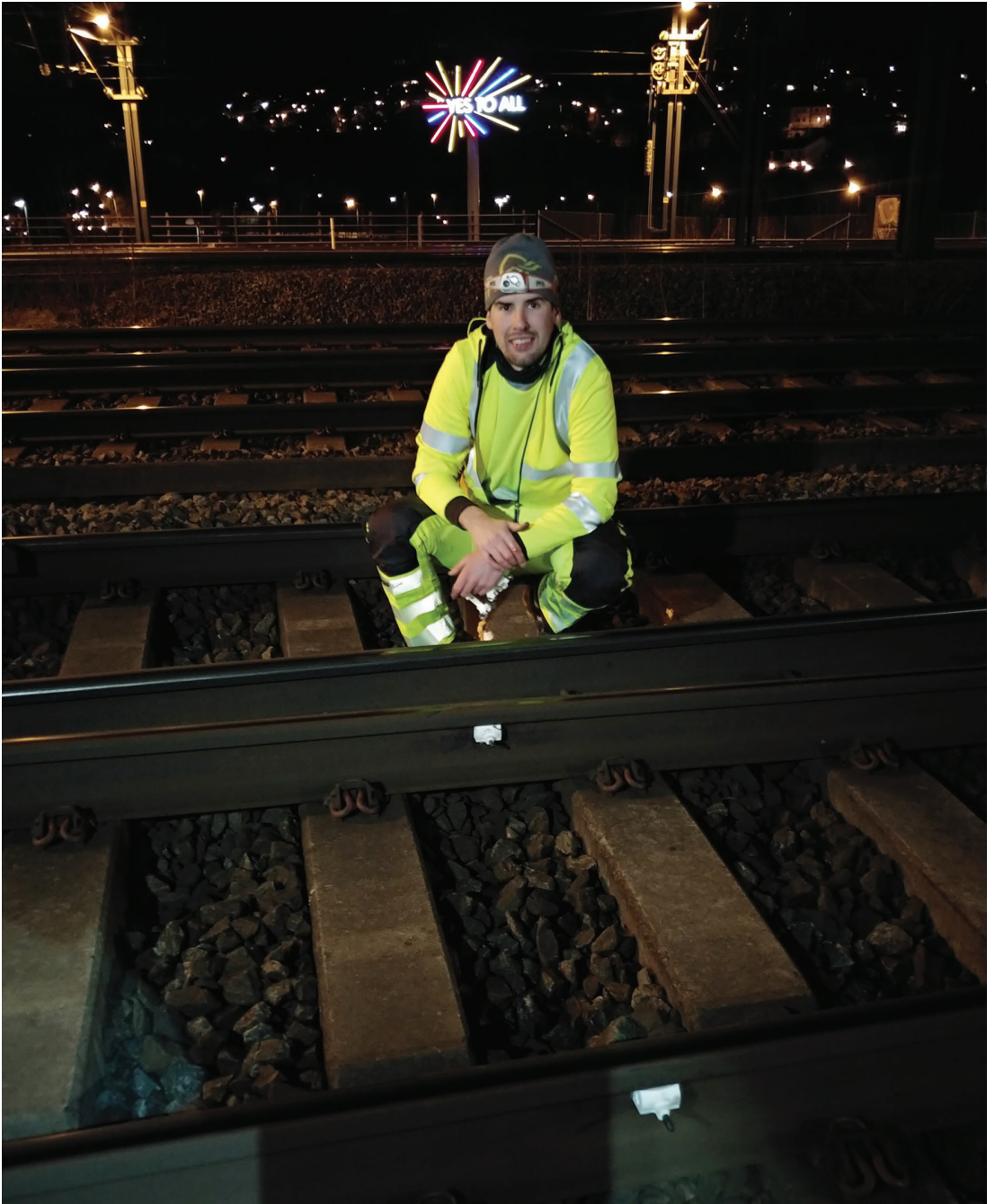


Figure C.16: Measurements in Norway (3)

ISBN 978-82-326-6121-3 (printed ver.)
ISBN 978-82-326-6488-7 (electronic ver.)
ISSN 1503-8181 (printed ver.)
ISSN 2703-8084 (online ver.)



NTNU

Norwegian University of
Science and Technology